Market Structure and Government Efficiency in Pandemics: Evidence from Nursing Home Networks

Roland Pongou[1], Ghislain Junior Sidie[1], Guy Tchuente[2*] and Jean-Baptiste Tondji[3]

[1]Dept. of Economics, University of Ottawa.
[2]Dept. of Agricultural Economics, Purdue University.
[3]Dept. of Economics, University of Texas Rio Grande Valley.
*Corresponding author(s). E-mail(s): gtchuent@purdue.edu;
Contributing authors: rpongou@uottawa.ca;
gsidi040@uottawa.ca; jeanbaptiste.tondji@utrgv.edu;

Abstract

How does market structure affect the efficiency and distributional impacts of the government policy response to health crises? To address this question, we examine the long-term care market in the early period of the COVID-19 pandemic in the United States, distinguishing between for-profit (FP) and not-for-profit (NFP) nursing homes. Using unique data on the social networks of over 11,000 nursing homes in 40 states, we show that FP nursing homes incurred more deaths from COVID-19 than NFP nursing homes. For the exploration of causal mechanisms, we calibrate a two-sector continuous-time individual-based mean-field model and estimate the efficiency of public health and safety interventions (PHSIs) in curbing the spread of COVID-19. We find that PHSI efficiency interacts significantly with the ownership status of a nursing home to determine COVID-19 death among residents: a one standard deviation increase in PHSI efficiency increases the death gap between FP and NFP nursing homes by around 23 percent relative to the mean. Analyzing possible mechanisms, we show that FP nursing homes have more difficulties adapting to PHSIs. Our analysis implies that policymakers should account for both market and network structures and their heterogeneity in experiencing uncertain shocks when designing optimal targeted interventions for future pandemics.

Keywords: Market structure, Government efficiency, Profits, Pandemics, Social networks, Nursing homes

JEL Classification: D85 , E61 , H12 , I18 , J14

1 Introduction

In a pandemic, governments face the complex problem of selecting optimal intervention strategies to cope with the adverse effects of the health crisis. These decisions are challenging because more stringent measures result in economic contraction, while laissez-faire policies likely lead to a high death toll. This paper is interested in the *efficiency* and the *distributional effects* of non-pharmaceutical public health and safety interventions (PHSIs) in all economic sectors.Using unique data on the social networks of nursing homes in the United States (U.S.), we focus on the differential behaviors and outcomes of for-profit (FP) and not-for-profit (NFP) nursing homes. First, using U.S. state-level PHSIs, we analyze the interplay between policy intervention, ownership structure, and COVID-19 death in nursing homes. Second, to understand the causal link and transmission mechanisms, we theoretically study lockdown interventions that optimize the trade-off between fatalities due to virus spread and economic costs in a pandemic that spreads through networks of physical contacts. Third, we calibrate our planning model of optimal lockdown to jointly quantify the governor's preference for PHSIs and the efficiency of these PHSIs at the state level. The preference for PHSI describes the trade-off between prioritizing health over short-term wealth accumulation during the COVID-19 pandemic. Finally, using estimated measures of PHSI efficiency, we explore the interplay between PHSI strategies, nursing home ownership status, and other characteristics that may have contributed to excess COVID-19 mortality rates in nursing homes. We also shed light on possible mechanisms driving our main findings.

Analyzing the distributional effects of contagion-reducing measures in the long-term care market is important for several reasons. It is well known that nursing facilities have borne the burden of COVID-19 mortality in several developed economies. For instance, as of June 1, 2021, nearly one-third of U.S. COVID-19 deaths were linked to nursing homes (Conlen et al., 2021); also, residents of nursing homes represented 81% of all reported COVID-19 deaths in Canada, and more than 50% in Sweden (Akhtar-Danesh, Baumann, Crea-Arsenio, & Antonipillai, 2022); and as of June 30, 2021, residents of nursing homes and long-term care facilities accounted for 74% of total COVID-19 deaths in Australia (Dykgraaf et al., 2021). Understanding how the pandemic has impacted the main long-term care providers could affect the sorting of individuals between nursing homes.

While nursing home facilities have been the most affected by the COVID-19 pandemic, there are significant disparities between nursing homes according to ownership status. Our data show that death rates were 28% higher among residents of FP nursing homes than among those of NFP nursing homes in the United States.[1] The factors explaining these inequalities have not been

[1]This observation is consistent with other studies. There have been concerns about poor health outcomes in nursing facilities, and FP status has often been suggested as a significant underlying factor (Bach-Mortensen, Verboom, Movsisyan, & Degli Esposti, 2021; Chen, Chevalier, & Long, 2021; Giri, Chenn, & Romero-Ortuno, 2021; Gupta, Howell, Yannelis, & Gupta, 2021; Spector, Selden, & Cohen, 1998).

widely studied. In this paper, we argue that FP nursing homes had difficulty adapting to public health and safety interventions (PHSI), leading to higher death rates among their residents compared to NFP nursing homes. Indeed, Figure 1 shows that as the death rate increased, which led the government to intensify PHSI measures, the mortality gap between FP and NFP nursing homes also increased. This observation is robust in different measures of PHSI. Although internal factors such as nursing home quality and socioeconomic status in the county could partially explain this gap, our analysis suggests that the differential effects of PHSI efficiency could also play a role. Motivated by this idea, we propose a framework for modeling the interaction between public and safety interventions during pandemics, ownership (or market) structures of nursing homes, and potential pandemic outcomes. Our model, which provides a micro-founded analysis of this interaction, also allows us to generate a measure of PHSI free from confounding factors and, therefore, allows a causal interpretation of the interplay between PHSI efficiency and ownership status in death rates. This analysis is important because exploring the factors affecting the structure of markets and their heterogeneity in experiencing uncertain shocks could help policymakers design optimal targeted non-pharmaceutical interventions for future pandemics.

We develop a two-sector version of the controlled epidemiological N-SIRD (Susceptible, Infected, Recovered, Deceased) agent-based model. The model incorporates a non-random network (N) of physical contacts and a variable that captures the government PHSI strategy. The economy's two sectors (or groups) could be differentiated with unique identifiers, such as demographic, institutional, geographic, and economic characteristics. In our planning problem, the PHSI strategy depends on the planner's tolerable infection incidence level (denoted $\iota \in [0, 1]$), which could depend on society's preferences. The mitigation policies are designed to reduce the level of contagion (below the incidence threshold ι) while also addressing the economic objectives and constraints of the two sectors of the economy. Also, we assume that being in lockdown does not entirely free an agent from potential contamination. Thus, we consider a PHSI efficiency parameter ($\theta \in [0, 1]$) to measure how effectively a PHSI strategy reduces contagion.

Although enforcing PHSI strategy could effectively reduce or prolong the contagion, it may also induce high socioeconomic costs. The latter include, among others, economic, human, and health costs.[2] To solve the planner's tradeoff problem, we first characterize the disease dynamics in our two-sector N-SIRD epidemiological model and obtain a solution under classical conditions. Our theoretical findings show that infection, recovery, and death rates at any given time are functions of the PHSI variable and its efficiency parameter, the initial network structure of contacts, and the exogenous epidemiological parameters. Second, we solve the planner's problem using optimal control

[2]For a recent discussion on the effects of enforcing control (e.g., lockdown) policies during the COVID-19 pandemic, see, e.g., Pestieau and Ponthiere (2022), Marquez-Padilla and Saavedra (2022), Di Porto, Naticchioni, and Scrutinio (2022), Caulkins et al. (2021), Cronin and Evans (2021), Federico and Ferrari (2021) and Palomino, Rodríguez, and Sebastian (2020).

theory and discuss conditions guaranteeing the existence of solutions. Each possible solution depends on the above exogenous variables (and parameters) of interest. We also find that the optimal size of the PHSI strategy decreases with PHSI efficiency for NFP nursing homes. However, the relationship between the optimal PHSI strategy and its effectiveness in FP nursing homes is ambiguous.[3]

We apply our model to the long-term care market in the U.S. in the early period of the COVID-19 pandemic.[4] In this country, we can differentiate nursing care providers by institutional ownership, which makes it suitable for applying our two-sector framework. Indeed, from the 11,395 unique skilled nursing facilities we observed from the data (Chen et al., 2021), about 69% are FPs and 31% are NFPs. On average, FP nursing homes tend to be more centrally located within the network of nursing homes than NFP nursing homes. Out of the 24,692 COVID-19 resident deaths reported during our period of study, about 74% (or 18,381) deaths come from FPs.[5] Of particular interest to our study is how the FP status of a nursing home interacts with PHSI (lockdown) efficiency to affect COVID-19 death among residents.[6]

We calibrate relevant parameters of our two-sector N-SIRD model and test our theoretical predictions using the unique U.S. nursing home networks data provided by Chen et al. (2021). Our calibration approach allows us to jointly estimate the value of the tolerable COVID-19 infection incidence level (ι) and the PHSI efficiency parameter (θ) for 40 U.S. states. The parameter ι estimates the U.S. state government's tolerable COVID-19 infection incidence, which by assumption represents the level at which the governor trades population health for short-term wealth accumulation. As such, a higher value of ι describes a less stringent containment measure similar to a laissez-faire policy (Gollier, 2020) and indicates the behavior of a wealth-leaning planner. The PHSI parameter θ estimates the state's preparedness for an effective or efficient lockdown (or PHSI) strategy. In other words, θ represents the extent to which a PHSI strategy can effectively curb the diffusion of the virus.

Based on a simulated minimum distance estimator (Forneron & Ng, 2018; Gertler & Waldman, 1992), our calibration-estimated results show great variation in ι and θ across U.S. states. Both range from almost zero to one. The

[3]In an early version of this manuscript, we explore this association in-depth using both simulations involving parameters calibrated for the early period of the COVID-19 pandemic and regression-based analyses.

[4]We note that our theory is general enough and can be applied more broadly. Data on nursing home networks were collected by the researchers of the "Protect Nursing Homes" project hosted by Yale University; networks are built using smartphone data. See Section 5 for a detailed data description.

[5]For additional statistics and facts on nursing homes' characteristics and COVID-19 fatalities, see, e.g., Chen et al. (2021), Ioannidis, Axfors, and Contopoulos-Ioannidis (2021) and Cronin and Evans (2022).

[6]In our application, we view a "lockdown policy" as a collection of costly preventive interventions that reduce social and work interactions. In addition to social distancing policies, a lockdown in nursing homes includes visitation restrictions imposed on visitors and non-essential healthcare personnel; such restrictions may not apply to compassionate care situations, such as end-of-life situations, as enforced by the U.S. Centers for Medicare & Medicaid Services from May 13, 2020, to September 17, 2020. A desirable PHSI strategy in the long-term care market should allow each provider to maintain its bottom line. In the best scenario, NFP nursing homes can break even while FP providers maximize profits.

average values of ι and θ are 0.33 ($s.d. = 0.22$) and 0.53 ($s.d. = 0.38$), respectively.[7] Using a regression-based analysis, we find that intensification of PHSIs, as represented by higher PHSI efficiency, tends to lead to fewer COVID-19 deaths in nursing homes. We also find that higher PHSI efficiency significantly increases the difference in COVID-19 deaths between FP and NFP nursing homes. Compared to a situation where PHSI efficiency is close to zero, a fully effective lockdown strategy increases the death differential between FP and NFP nursing homes by 1.29, representing 59 percent of the mean. A one standard deviation increase in PHSI efficiency raises the death gap by around 23 percent relative to the mean. These effects are large and statistically significant. Furthermore, we find that nursing homes that are more central in the network record more COVID-19 deaths, and their vulnerability increases significantly with PHSI efficiency. All these results are robust when controlling for an array of nursing home-level and U.S. state-level characteristics, such as overall nursing home quality, county socioeconomic status, the OxCGRT indexes that capture government PHSIs during the COVID-19 pandemic, and county fixed effects.[8] in explaining resident COVID-19 deaths in nursing facilities.

Our findings emphasize the pivotal role of PHSIs in elucidating the observed divergence in COVID-19 mortality rates between FP and NFP nursing homes during the pandemic. We propose mechanisms through which variations in PHSI efficiency levels may have benefited NFP homes over FP homes in pandemic management. This analysis indicates that increasing PHSI efficiency levels decreases rule violations in nursing homes but exacerbates shortages in aid and nursing staff, notably impacting FP homes. Greater PHSI efficiency intensifies pressure to reduce mobility, exacerbating nurse shortages, especially for FP homes, which may be highly dependent on part-time staff. Consequently, this scarcity of nursing staff may lead to higher mortality rates in FP homes due to challenges in meeting safety standards and increased violations of rules.

We analyze some other possible mechanisms. There are potential issues of moral hazard or resource constraints in FP homes. Given the absence of insurance products to protect nursing home owners from pandemics, FP homes may face financial constraints during increased staff demand, impeding standards improvements. The rapid adoption of numerous PHSIs by policymakers during the pandemic may have imposed an unduly heavy burden on compliance for FP homes, resulting in a relatively higher incidence of rule violations, possibly

[7] In an early version of this manuscript, using regression-based analysis, we found that state-level differences in demographic and political characteristics can explain variations in PHSI efficiency levels. These factors include, among others, policy responses during the COVID-19 pandemic, the party affiliation of the governor, the approval rate of the governor, the state's OxCGRT indexes, the state's geographic location, the state GDP growth, the distribution of nursing homes' ownership in the state, and the number of COVID-19 deaths in the state.

[8] Cronin and Evans (2022) used CMS nursing home data and the COVID-19 Tracking Project to examine whether the nursing home quality predicts U.S. COVID-19 mortality. The authors find that higher quality nursing homes, as measured by "CMS's overall five-star rating", have significantly fewer resident COVID-19 deaths from May 24th through September 2020. We complement this study by highlighting the role of the U.S. nursing home networks and PHSI efficiency

indicative of moral hazard. Indeed, we find that FP nursing homes had difficulties complying with lockdown measures. We find that these difficulties are explained by staff shortages during the pandemic. Targeted monitoring strategies are recommended to improve the level of implementation of the rules. We also believe that addressing the incomplete insurance market for FP homes in pandemic resource allocations is crucial, although the methodology for such allocation lies beyond the scope of this paper.

The remainder of this paper is organized as follows. Section 2 discusses our contribution to the literature. We explore some patterns in relationships between PHSI strategies and the FP vs NFP COVID-19 death gap in Section 3. In Section 4, we present a two-sector N-SIRD model with lockdown and planning problem. Section 5 offers an application to U.S. nursing homes. In particular, Section 5.1 illustrates how PHSI efficiency affects optimal PHSI and disease dynamics in nursing homes. Section 5.2 estimates the PHSIs using U.S. nursing home data. Section 5.3 provides an empirical regression-based analysis of the relationship between COVID-19 deaths and the structural measure of PHSI efficiency, and Section 6 concludes. The Appendices contain proofs of propositions, additional figures, and tables.

2 Contribution to the Related Literature

Our paper contributes to the literature that combines economics and epidemiology to address various issues. In modeling a pandemic, we incorporate a non-random social network as in Pongou, Tchuente, and Tondji (2022, 2023) but differ from these latter studies in two important respects. First, the model in Pongou et al. (2022, 2023) does not incorporate PHSI efficiency; it implicitly assumes that the lockdown ultimately reduces the contagion (that is, $\theta = 1$). Leaving θ different from 1 is consistent with some early studies, although our model and its applications to nursing home networks differ significantly. Second, in contrast to Pongou et al. (2022, 2023), we split the population into two sectors based on one key variable—FP status (or "nursing home ownership" in our application). In this sense, our work is related to recent studies investigating the role of individual characteristics such as race, sex, and age in pandemic fatalities in epidemiological models (Debnam Guzman, Mabeu, & Pongou, 2022; Gebhard, Regitz-Zagrosek, Neuhauser, Morgan, & Klein, 2020; Gollier, 2020). However, our scope, analysis, and policy implications differ from those of these previous works. Regarding the analysis, we provide a simulation-based estimation of the PHSI efficiency parameter θ in a network-based epidemiological and economic model. Furthermore, we study the effect of the tolerable incidence of infection by planners on the efficiency of PHSI during the COVID-19 pandemic.

The epidemiological framework we use to model the planning problem is a continuous-time individual-based mean-field model, which belongs to the class of theoretical approaches for epidemic modeling on undirected heterogeneous networks. Pastor-Satorras, Castellano, Van Mieghem, and Vespignani

(2015) provide a review of these epidemiological models, Boucekkine, Carvajal, Chakraborty, and Goenka (2021), Debnam Guzman et al. (2022), Eichenbaum, Rebelo, and Trabandt (2022), Pongou et al. (2022), Fernández-Villaverde and Jones (2022), Pongou et al. (2023) and Nganmeni, Pongou, Tchantcho, and Tondji (2022) highlight the recent economic contributions to the COVID-19 pandemic.[9] Another contribution by Makris (2021) also extends the classical susceptible-infected-recovered (SIR) model by incorporating heterogeneity in infection-induced mortality rates at the population level. Although our models share some ingredients (e.g., the lockdown variable), our paper addresses a different issue using a distinct modeling approach.

Our study also contributes to the growing literature seeking to understand the results of poor pandemic outcomes in the long-term care market and how the government interventions influenced the outcome (Bach-Mortensen et al., 2021; Dykgraaf et al., 2021; Giri et al., 2021; Gupta et al., 2021; Gutierrez & Rubli, 2021; Herz, Kistler, Zehnder, & Zihlmann, 2024; Londoño-Vélez & Querubin, 2022; Zhao, Yao, Thomadsen, & Wang, 2024; **?**). We analyze the role of PHSI efficiency in setting optimal confinement strategies in nursing facilities during a pandemic. Using simulations and regression-based analysis of U.S. nursing home networks data, we show that U.S. state governors' response policies, combined with state-level PHSI efficiency, contribute significantly to the dynamics of COVID-19 outcomes in U.S. nursing homes, and this effect largely depends on their for-profit status.[10] Our analysis differs from other studies in providing a micro-founded model to understand how nursing home ownership affects COVID-19 outcomes. Our analysis also shows that PHSI efficiency is essential in explaining the COVID-19 death differential between FP and NFP nursing homes. Additionally, due to the network structure of our data, our empirical analysis controls for variables (e.g., network centrality index) that are not included in other recent studies investigating the effect of nursing home ownership on the outcomes of COVID-19. Our findings and those of previous studies could help planners develop effective mitigation strategies against current and future pandemics.

[9] Our model also complements other economic studies that examine the diffusion of innovation or contagion in non-mean-field-based network models; see, e.g., Ballester, Calvó-Armengol, and Zenou (2006), Lloyd, Valeika, and Cintrón-Arias (2006), Young (2009), Young (2011), Pongou and Serrano (2013), Banerjee, Chandrasekhar, Duflo, and Jackson (2013), Buechel, Hellmann, and Klößner (2015), Battiston and Stanca (2015), Pongou and Tondji (2018), and Galeotti, Golub, and Goyal (2020).

[10] Our analysis also complements earlier studies showing that demographic, geographic, and macroeconomic characteristics explain differences in COVID-19 outcomes between countries and cities. For a cross-country comparison, we refer to Assob-Nguedia, Dongo, and Nguimkeu (2020), Nguimkeu and Tadadjeu (2021), Bartscher, Seitz, Siegloch, Slotwinski, and Wehrhöfer (2021), and Fernández-Villaverde and Jones (2022).

3 PHSI and COVID-19 Death Gap in U.S. Nursing Homes

This section documents the cross-relationship between the type of ownership of nursing homes, the level of stringency of the public health and safety interventions to the COVID-19 pandemic, and COVID-19 deaths in U.S. nursing homes. The analysis runs through four main sections. First, we briefly review the data describing the institutional, economic, and partial representation of the U.S. nursing home network structure. Second, we briefly introduce a set of government responses at the onset of the COVID-19 pandemic. Third, we document a persistent COVID-19 death gap between FP and NFP nursing homes. Fourth, we evaluate the extent of the contribution of different factors to the COVID-19 death gap between FP and NFP.

3.1 Structure of Nursing Homes

3.1.1 Economics

Nursing homes provide short-term rehabilitative care and long-term custodial services for individuals unable to live independently. In the U.S., providers of nursing home services are delivered by a combination of for-profit, not-for-profit, and public providers, and they are paid by third-party, largely government payers through Medicare and Medicaid programs and private insurance companies (Gupta et al., 2021). FP providers are commonly known as private adult social care firms operating on a for-profit basis; NFPs are known as providers registered not-for-profit or charitable organizations; and public providers are understood as those operated by the central or local government. In our study, we consider public providers of nursing care as NFPs. In the U.S., about 70% of nursing home providers are FP.[11] The rates set by government payers are adjusted for patient complexity and are non-negotiable such that providers act as price-takers in the U.S. long-term care market relative to other healthcare sectors. The nature of institutional care offered by nursing home providers requires high fixed costs, making the occupancy rate a key driver of profitability. Additionally, labor and, precisely, nursing staff represent providers' most prominent elements of operating costs and constitute a significant component of the quality of services in most nursing homes (Gupta et al., 2021; O'Neill, Harrington, Kitchener, & Saliba, 2003). Given the pay structure in the U.S. nursing home markets, it is difficult for patients to rely on price as a relevant indicator of service quality. There is a consensus that reputation contributes greatly to the demand for nursing home services. Therefore, FP providers are induced to optimally choose between capital investments (e.g., buildings) and labor (for example, high ratios of nursing staff to patients) to maintain their reputation and profits. As documented by Gupta et al. (2021) and others, such actions can produce detrimental effects on patient health outcomes, such as the higher number of COVID-19 deaths

[11] For additional information on nursing home ownership, see Bach-Mortensen et al. (2021).

reported recently in FP nursing homes (Akhtar-Danesh et al., 2022; Conlen et al., 2021; Dykgraaf et al., 2021).

3.1.2 U.S. Nursing Home Networks

In our study, we exploit the social network structure of nursing homes collected by the staff of the "Protect Nursing Homes" project at the onset of the COVID-19 pandemic.[12] After the national lockdown on nursing home visits introduced by the U.S. Federal government on March 13, 2020, the members of the "Protect Nursing Homes" project used geolocation data for about 50 million smartphones during the 11-week study period to build the U.S. nursing home networks. They observed that 5.1% of smartphone users (approximately 501,503 staff and contractors) who visited a nursing home for at least 1 hour also visited another facility during the 11-week study period—even after visitor restrictions were imposed. In the nursing home network for each U.S. state, nodes denote individual nursing facilities. A connection is established between two nursing homes, say i and j, if a staff from the nursing home i visited the nursing home, j, for at least 1 hour. The intensity of the connection between two nursing homes depends on the number of smartphones observed in both homes. Following the above description, a PHSI mandating a lockdown policy in a nursing home could include a combination of restrictions on family visits, prohibition on admitting new residents to the nursing home, or transferring residents from hospitals or other care homes to the nursing home. Given the lack of accurate death data at the beginning of the COVID-19 pandemic, we use the data from the Centers for Medicare & Medicaid Services Data (CMS) from May 31 to August 16, 2020.[13]

3.2 PHSI – The OxCGRT indexes

During the pandemic, several studies tracking planners' actions towards mitigating the pandemic (Hale et al., 2021) were performed. The Oxford COVID-19 Government Response Tracker (OxCGRT) is a project from Oxford University. They track national and, for some countries (e.g., the U.S.), subnational governments' policies and interventions across a standardized series of indicators. The OxCGRT's project created a suite of composite indexes, including the stringency index (SI), the containment and health index (CHI), the more comprehensive government response index (GRI), and the economic support index (ESI). The index SI exclusively assesses the extent of closure and containment policies. In addition to the indicators defining SI, the index CHI includes health system policies such as public information campaigns, testing, and contract tracing policies. ESI provides a holistic measure of financial assistance to households, and GRI is an overall measure of the government's PHSI during

[12] For more information on the "Protect Nursing Homes" project, we refer to the website https://protectnursinghmes.org, and Chen et al. (2021).

[13] COVID-19 nursing home data of the CMS are available at https://data.cms.gov/covid-19/covid-19-nursing-home-data.

the COVID-19 pandemic.[14] Along with other key variables used in the study, we summarize in Table 1 the descriptive statistics of the OxCGRT indices.[15]

Table 1 is about here

3.3 Evidence of the FP vs. NFP COVID-19 Death Gap

As highlighted in the Introduction, nursing homes worldwide have borne a significant share of fatalities during the COVID-19 pandemic. Although the nature of the pandemic could be a simple reason, studies show that internal and external factors in nursing homes have significantly aided in COVID-19-related deaths in nursing homes. Existing literature, as noted by Cronin and Evans (2022), Bui (2020), and Bui (2020), identifies several protective and contributing factors. For instance, higher-quality nursing homes, measured by the CMS's overall five-star rating, exhibit significantly lower COVID-19 death rates. Staffing levels also played a pivotal role in determining the incidence of COVID-19 deaths (Gorges & Konetzka, 2020; Harrington et al., 2020). Other contributing factors associated with COVID-19 mortality include county COVID-19 incidence, nursing home racial composition, and primarily, ownership type, precisely, FP and NFP (Bach-Mortensen et al., 2021; Chen et al., 2021; Gorges & Konetzka, 2020; Gupta et al., 2021; Li, Cen, Cai, & Temkin-Greener, 2020). From these previous studies, ownership of nursing homes is a critical factor in explaining the severity of the COVID-19 pandemic in nursing homes. In this section, we use existing data collected during the early period of the COVID-19 pandemic to provide evidence of the interaction of public health and safety interventions and the ownership of nursing homes on COVID-19 deaths in the U.S. nursing home network.

3.3.1 PHSI indexes and COVID-19 death gap

We illustrate in Figure 1 the gap in COVID-19 deaths between FP and NFP nursing homes using the PHSI indexes. It is without any doubt that for-profit and not-for-profit nursing homes experience different death dynamics, with a greater number of deaths in FPs. As one may expect, the stringency of each PHSI is positively correlated with the severity of the pandemic fatalities. However, although PHSIs are likely uniform within states and nursing homes, the resulting effects are dissimilar since, from Figure 1, the COVID-19 death gap between FP and NFP nursing homes seems to widen with the increasing intensity of government interventions.

Figure 1 about here

[14] For an update on these government responses, we refer to the work of Cheng et al. (2024). Our analysis are carried out at the state level and using early COVID-19 pandemic data (see Baumeister, Leiva-León, and Sims (2024); Callaway and Li (2023)) who work with similar data.

[15] This table also presents the descriptive statistics of nursing facilities' and U.S. states' characteristics. We present the summary statistics for the entire sample and the subsamples of FP and NFP nursing homes.

During the COVID-19 pandemic, most PHSIs aimed to foster social distancing behaviors, compliance with lockdown strategies, and an increase in the supply of face masks, hand sanitizers, PPE, and ventilators in hospitals, and boosting resources for cure and vaccines. However, at the onset of the pandemic, without a full scope of the virus, most governments implemented different types of lockdown policies aiming to curb individuals' mobility. The ownership structure of nursing homes in the United States exhibits some heterogeneity, with for-profit entities comprising over 70 percent of care providers. This domination of FP nursing homes is the result of mergers and acquisitions, consolidation, and other changes in ownership structures of U.S. care facilities. Given the resources and cost-minimizing strategies that these nursing facilities develop to provide their services, we may expect different mobility dynamics in response to the implementation of social distancing and lockdown measures during the COVID-19 pandemic. To explore this, we incorporate workplace visits, as captured by Google's Community Mobility Reports (CMR, 2020), and the overall quality of nursing homes as control variables. By doing so, we aim to elucidate the relationship between COVID-19 deaths and the intensity of public health and safety interventions.

Table 2 about here

The regression results presented in Table 2 reveal a notable trend: greater value of PHSI indexes correlates with reduced mortality rates, holding mobility constant. Furthermore, factors such as CMS overall quality rating, nursing home centrality, county socioeconomic status, and PHSI indexes collectively absorb the influence of ownership type in explaining variations in death rates across nursing homes. However, the statistical insignificance of the interaction term between ownership and proxy variable for mobility ownership type prompts a natural question: What role do governmental responses play in mitigating or exacerbating the disparate impact of ownership on COVID-19 death?

3.3.2 Oaxaca-Blinder decomposition

The descriptive analysis in Table 1 and the data depicted in Figure 1 highlight the inequality in COVID-19 deaths between FP and NFP nursing homes. To delve deeper into this disparity, we employ the Oaxaca-Blinder decomposition method to elucidate the key factors that may have contributed to this COVID-19 death differential by ownership of U.S. nursing homes. Table 3 provides the results of this decomposition thanks to the multiple regression model that disentangles the COVID-19 death inequality into various internal and external factors. The results indicate that the difference in the mean predicted COVID-19 deaths between FP and NFP nursing homes is predominantly and significantly influenced by variations in observable characteristics. These include CMS overall quality rating, nursing home centrality, county SES, and PHSI indexes. When considering nursing homes with identical characteristics in both the FP and NFP groups, any remaining COVID-19 death inequality may be attributed to the differential effects of these characteristics

and unobserved factors not included in the model. However, this remaining portion is statistically insignificant globally, although, as in the specification described in column (4) of Table 3, it comprises a positive and statistically significant contribution from network centrality and a negative or non-statistically significant contributions from PHSI indexes and other variables.

Table 3 about here

Motivated by all the evidence above, we propose a complementary structural epidemiological and economic framework that a modeler can use to support a causal analysis of the differential effect of the interaction of government interventions and care provider ownership (and other potential mechanisms) on deaths during health crises like COVID-19. The model we are proposing in Section 4 captures government interventions while accounting for the heterogeneity of nursing homes. Thus, we can provide a better understanding of the interplay between ownership structures, PHSI indexes, and pandemic outcomes. These relationships hold significant implications for policy formulation and healthcare management of pandemics such as COVID-19.

4 A two-sector N-SIRD model with PHSI

We develop an epidemiological and economic model to address the problem of a planner who wants to mitigate the health and economic burden of a viral respiratory infection affecting society without vaccines and treatments. The infection spreads through an undirected weighted and symmetric network of physical contacts that we denote by $\mathcal{M}$, with its adjacency matrix being $(\mathcal{M}_{i,j})$, where $\mathcal{M}_{ij} = \mathcal{M}_{ji} \in [0, \infty)$ represents the *weight* or *intensity* at which agents (or individuals) i and j are connected in $\mathcal{M}$, with $\mathcal{M}_{ij} = 0$ if $i = j$. Time t is continuous, $t \in [0, \infty)$. Contrary to the N-SIRD model with the lockdown proposed by Pongou et al. (2023), agents are divided into two sectors (or groups) A and B. We denote by N^g, $g \in \{A, B\}$, the initial number of agents in sector g. The two sectors can be differentiated with unique identifiers, including demographics, institutional, geographic, or economic characteristics.[16] There are no vital dynamics so that the total population $N(t) = N^A(t) + N^B(t) = N \geq 1$ for all t. Agents are subdivided into susceptible (S), infected (I), recovered (R), and deceased (D),

$$S(t) + I(t) + R(t) + D(t) = N.$$

At each period t, each agent i is in each of the four different compartments with the following probabilities: $s_i(t) = P(i \in S)$, $x_i(t) = P(i \in I)$, $r_i(t) = P(i \in R)$, and $d_i(t) = P(i \in D)$, with $s_i(t) + x_i(t) + r_i(t) + d_i(t) = 1$.

[16] Indeed, following Gollier (2020), one can partition individuals or agents into multiple sectors, extending the N-SIRD to a multi-sector N-SIRD model. Given the complexity of modeling pandemics through the lens of mean-field network-based approaches (Pastor-Satorras et al., 2015), we consider two sectors for simplicity and applicability.

4.1 Incorporating the planning intervention measures

We incorporate a lockdown variable to capture the fact that a planner might decide to reduce the spread of the infection by enforcing a lockdown policy or public health and safety intervention (PHSI). The lockdown strategy reduces the spread of infection by modifying the existing social network structure, $\mathcal{M}$. Let L denote the lockdown state that the planner controls and $l_i(t) = P(i \in L)$ denote the probability that a random agent i is sent into lockdown at period t, with $l_i(t) = 1$ designating complete lockdown and $l_i(t) = 0$ no lockdown. Following several studies, we assume that the lockdown is only partially effective in eliminating the transmission of the virus since some contacts will still happen in the population even under a complete economic lockdown. We denote as θ, the **PHSI efficiency parameter**, with θ ($\theta \in [0, 1]$). The variable θ is the PHSI efficiency parameter, which by definition is the rate at which the PHSI effectively reduces infection in the social network, $\mathcal{M}$. When there is no ambiguity, we remove the continuous time parameter t in our variables of interest.

4.2 Disease dynamics

Susceptible agents may become infected by being in contact with infected agents at a constant passing rate $\beta \in [0, 1]$. Agent i's infection probability is equal to the likelihood that they are susceptible (s_i) and not sent into complete lockdown ($1 - \theta l_i > 0$) multiplied by the probability that a neighbor j is infected ($x_j > 0$) and is not sent into complete lockdown ($1 - \theta l_j > 0$), scaled by the connection intensity between i and j ($\mathcal{M}_{ij} > 0$) and the contact rate β. Therefore, the susceptible probability of an agent i evolves according to the law of motion:

$$\dot{s_i} = -\beta s_i(1 - \theta l_i) \sum_{j \in N} [\mathcal{M}_{ij}(1 - \theta l_j)x_j]. \tag{1}$$

Agents who move from susceptible to infected recover at rate γ or die at rate κ, with γ and $\kappa \in [0, 1]$. The law of motion of agent i's infection probability is then

$$\dot{x_i} = \beta s_i(1 - \theta l_i) \sum_{j \in N} \mathcal{M}_{ij}(1 - \theta l_j)x_j - (\gamma + \kappa)x_i. \tag{2}$$

For each $i \in N$, let $X_i(t) = (x_i(t), s_i(t), r_i(t), d_i(t))^T$ denote the health characteristics of agent i' in the population in period t, where T means "transpose". Given the lockdown profile $l = (l_i)_{i \in N}$, equations (1) and (2), the law of motions of recovery probability $\dot{r_i} = \gamma x_i$ and death probability $\dot{d_i} = \kappa x_i$, the constraint $s_i + x_i + r_i + d_i = 1$, with the initial value point $X_i(0) = (x_i(0), s_i(0), r_i(0), d_i(0))$ satisfying $x_i(0) \geq 0$, $s_i(0) \geq 0$, $r_i(0) \geq 0$ and $x_i(0) + s_i(0) + r_i(0) + d_i(0) = 1$ constitute the system (ODE) describing a typical representation of an individual-based mean-field model for epidemic modeling on networks. We refer interested readers to Pastor-Satorras et al. (2015) for a detailed survey of epidemic modeling in networks. Proposition 1 demonstrates the existence of a unique solution for the system (ODE).

Proposition 1 *The system (ODE) admits a unique solution.*

Below, we formalize the planning problem.

4.3 The planning problem

In the face of the pandemic, the planner's main objective is to contain the contagion. When there is no cure or vaccine, most planners choose nonpharmaceutical interventions, including lockdown and social distancing protocols. Given the social costs such mitigation policies could drive into society, planners are left to trade between economic prosperity and saving lives. Several factors could guide planners in adopting reasonable pandemic mitigation strategies. In line with their objectives, the planner decides to curb the spread of contagion by containing the relative rate of new cases in the population. Following Pongou et al. (2023), using the differential equation that describes the evolution of infection probability $\dot{x_i}$ in the system (ODE), the planner aims to select a lockdown policy $l = (l^A, l^B)$, where $l^A = (l_i)_{i \in A}$ and $l^B = (l_i)_{i \in B}$, such that:

$$\dot{x_i} \equiv \dot{x_i}(l) \leq \iota, \ \iota \in [0, 1]. \tag{3}$$

The threshold, ι, is our second parameter of interest and represents the planner's tolerable infection incidence. The latter highlights their willingness level to balance health and economic resilience during the pandemic. Then, the pair (ι, θ) represents the pandemic's **PHSI profile**.[17] A health-leaning planner does not support higher tolerable infection incidence and undertakes more PHSI strategies than wealth-leaning planners. However, given the PHSI efficiency parameter θ, health-leaning planners with the same tolerable infection incidence level, ι, may undertake different PHSI decisions. For instance, health-leaning planners may enforce fewer PHSIs when these strategies are more likely to be effective in curbing the contagion in their constituencies. At any given period t, each agent i possesses a capital level k_i, and a labor supply $h_i \equiv h_i(s_i, x_i, r_i, d_i, l_i)$. We assume that h_i is non-decreasing in the likelihood of being susceptible and recovered: $\frac{\partial h_i}{\partial s_i} \geq 0$ and $\frac{\partial h_i}{\partial r_i} \geq 0$. In contrast, h_i is non-increasing in the likelihood of being infected and deceased, and h_i is also non-increasing in lockdown strictness: $\frac{\partial h_i}{\partial x_i} \leq 0$, $\frac{\partial h_i}{\partial d_i} \leq 0$, and $\frac{\partial h_i}{\partial l_i} \leq 0$. It is reasonable to assume that an agent who is working despite being infected produces less compared to an otherwise identical agent who is healthy. Without loss of generality, we assume that capital is constant over time ($k_i(t) = k_i$, for each period t), and labor is a variable input in the production function. Capital combines with labor to generate output, y_i, based on a production function: $y_i \equiv y_i(k_i, h_i) = y_i(k_i, s_i, x_i, r_i, d_i, l_i)$. We assume that y_i is continuous and differentiable in each input variable. With the above information,

[17] Note that the planner can "choose" the tolerable infection based on society's preferences. Our study assumes that it is constant and independent of the time: $\iota(t) = \iota \geq 0$, for each t. A natural extension could consider varying ι throughout the evolution of the pandemic.

agent i's surplus function (or economic profit), Π_i, is given as:

$$\Pi_i(k_i, h_i) = p_i y_i(k_i, h_i) - w_i h_i(s_i, x_i, r_i, d_i, l_i) \equiv \Pi_i(k_i, s_i, x_i, r_i, d_i, l_i), \quad (4)$$

where p_i and w_i stand for agent i's unit price of output and cost of labor, respectively. We assume that the function Π_i is jointly concave in the variables $(k_i, s_i, x_i, r_i, d_i, l_i)$ for all $i \in N$. The latter assumption is also guaranteed if we assume that the revenue function $p_i y_i$ (or simply the production function, y_i) is jointly concave in its variables, and the labor cost function $w_i h_i$ (or simply the labor supply, h_i) is jointly convex in its variables. Given the lockdown profile $l = (l^A, l^B) \in [0,1]^n$, the aggregate surplus is

$$\mathcal{S}(k, s, x, r, d, l) = \sum_{i \in N} \Pi_i(k_i, s_i, x_i, r_i, d_i, l_i). \quad (5)$$

Mitigation measures during pandemics could produce successful results with unintended social consequences. While they can reduce the contagion and health burden, they may drive other issues like massive job quitting, supply chain uncertainty, civil protests, and economic recession, among many others.[18] To minimize the social costs of lockdown, the planner desires all agents to stay afloat and provide essential economic services. For these reasons, planners aim to implement lockdown protocols that enable agents to remain as close to their pre-pandemic productivity levels as possible. There might be some basic level of surplus, say Π^g, for each sector $g \in \{A, B\}$, that agents should enjoy even under severe lockdown policies. We denote the set of such economic constraints by (EC). For instance, one can assume that for any lockdown profile $(l_i)_{i \in N}$, it holds that:

$$\text{(EC)}: \begin{cases} \underline{\Pi}^A \leq \Pi_i(k_i, s_i, x_i, r_i, d_i, l_i) \leq \overline{\Pi}^A, \text{ for all } i \in N^A, \text{ and} \\ \underline{\Pi}^B \leq \Pi_i(k_i, s_i, x_i, r_i, d_i, l_i) \leq \overline{\Pi}^B, \text{ for all } i \in N^B, \end{cases}$$

where $\underline{\Pi}^A$, $\overline{\Pi}^A$, $\underline{\Pi}^B$, and $\overline{\Pi}^B$ are all real numbers. Using optimal control theory, and given that for each $i \in N$, $s_i(t) = 1 - x_i(t) - r_i(t) - d_i(t)$, we can express agent i's net surplus as $\Pi_i\left(k_i, s_i(t), x_i(t), r_i(t), d_i(t), l_i(t)\right) \equiv \Pi_i\left(k_i, x_i(t), r_i(t), d_i(t), l_i(t)\right)$, and write the planner's problem as:

$$\begin{array}{ll} \underset{l=(l^A, l^B)}{\text{Maximize}} & \sum\limits_{i \in N} \int\limits_0^\infty e^{-\delta t} \Pi_i\left(k_i, x_i(t), r_i(t), d_i(t), l_i(t)\right) dt \\ \text{subject to} & \dot{x_i}(t) \leq \iota, \ i \in N \\ & \dot{r_i}(t) = \gamma x_i(t), \ i \in N \\ & \dot{d_i}(t) = \kappa x_i(t), \ i \in N \\ & l_i(t) \in [0,1], \ i \in N, \\ & \text{(EC) and initial conditions } X(0), \end{array} \quad (6)$$

[18] A recent evidence is a case of the Zero COVID-19 policies in China (Fuxian et al., 2022).

where δ is the planner's discount rate. The state variables, s, x, r, and d in the planning problem depend on the control (or lockdown) variable l. The planner's objective function in (6) shares similarities with several other works that develop macro-epidemic models in which the planner chooses the lockdown policy to maximize the present discounted value of aggregate real income (or revenue) net of loss of lives. Like these studies, our lockdown policy affects commuting flows, disease, and economic dynamics. Unlike these previous studies, we follow Pongou et al. (2023) and consider the tolerable infection incidence parameter ι, which provides an alternative to subtracting the monetary value of loss of lives from aggregate real income. A wealth-leaning planner displays a high value of ι and is willing to tolerate more loss of lives (and therefore less strict PHSI strategies) for short-term surpluses than a health-leaning planner.[19] It follows that the choice of ι by the planner affects the lockdown profile $l(t)$ and the disease dynamics through the system (ODE) and (3). Similarly, the lockdown profile $l(t)$ impacts the aggregate surplus and the social network structure through the system (ODE) and (5). The following result holds.

Proposition 2 *The planning problem in (6) admits a solution.*

The following section uses relevant data from the social care sector, including nursing homes and long-term care markets, to empirically evaluate the PHSI profiles (ι, θ) in our theoretical framework for U.S. states.

5 Estimation of the PHSI profile (ι, θ) in U.S. nursing homes models

The results in Section 3 present evidence of the COVID-19 death differential between FP and NFP nursing homes, with PHSI differences as a significant contributing factor. In this section, we calibrate the general model in Section 4 to the U.S. nursing home economy during the ban on nursing visits in the early days of the COVID-19 pandemic.

5.1 The two-sector U.S. nursing homes model

5.1.1 Nursing home ownership and economic constraints

As previously described, the structure of the long-term care market in the U.S. enables us to differentiate nursing homes (or agents in our theoretical framework) by ownership. Therefore, sector A represents FP nursing homes, and sector B comprises NFP nursing homes, including public providers. In the interest of consistency with previous notations, "nursing home" i (which naturally consists of a set of individuals) is equivalent to "agent" i. Thus,

[19] Following our approach, one can avoid the difficult problem of giving a monetary value to life. See also Pindyck (2020) and Bosi, Camacho, and Desmarchelier (2021) for a similar concern. An appeal of this approach is that it allows the planner to calibrate mitigation policies with the contagion level that society can tolerate.

the parameter s_i, which describes agent i's susceptibility probability, can be interpreted as the nursing home i's susceptibility rate. A similar interpretation holds for infection, recovery, death, and PHSI (or lockdown) variables. Given the institutional status of the nursing home ownership, under a desirable lockdown policy, nursing homes in sector A seek to maximize profits, and the following holds for nursing homes in sector B:

$$\Pi_i(k_i, s_i, x_i, r_i, d_i, l_i) = 0, \text{ for all } i \in N^B. \tag{7}$$

Then, we can rewrite the planning problem in (6) by setting the economic constraints (EC) for NFP nursing homes as in (7). We use data on U.S. nursing homes to estimate the COVID-19's PHSI profile (ι, θ) in U.S. states. Using these estimated values, we proceed to a causal evaluation of the interplay between ownership structures, governmental interventions, and pandemic outcomes.

5.1.2 Calibration of production functions

In line with the nursing home data, we assume that a Cobb-Douglas production function can approximate output (or care services) in a nursing home (Pongou et al., 2023). For simplification, we consider that capital is constant over time, i.e., for each $i \in N$, $k_i := k_i(t) = K_i$, for all t. We also approximate labor supply as a linear function of lockdown as follows:

$$h_i = 1 - \theta l_i, \ i \in N. \tag{8}$$

Then,

$$y_i = K_i^{\alpha_i}(1 - \theta l_i)^{1-\alpha_i}, \ i \in N, \ \alpha_i \in [0, 1]. \tag{9}$$

In (9), α_i is the capital-output elasticity, and $1 - \alpha_i$ is the labor-output elasticity. To estimate the elasticity α_i, we consider y_i as the total number of residents who receive care (proxies the nursing home i's output), k_i as the total number of beds (proxies the nursing home i's capital), and h_i as the number of occupied beds (proxies the nursing home i's labor supply). The functions h_i in (8) and y_i in (9) satisfy the standard conditions mentioned in Section 4. In Appendix A.3, we extend the theoretical derivation of the planning problem, which proves helpful in our simulations. Given the above specifications for the labor and the production function, Proposition 3 and Remark 1 below provide simple comparative static analyses between the lockdown and the PHSI efficiency parameter θ for FPs and NFPs, respectively.

Proposition 3 *The optimal lockdown probability decreases with the PHSI efficiency level θ for NFP nursing homes.*

Remark 1 While a negative monotonic relationship exists between the optimal lockdown and PHSI efficiency for NFP nursing homes, this is not true for FP nursing

homes. Appendix A.4 provides an insight into the ambiguous relationship between the two variables for FP nursing homes under certain conditions. These conditions require changing the planner's objective function (the discounted sum of profits for nursing homes) following a slight relaxation of some constraints to be unresponsive to the PHSI efficiency parameter θ at the equilibrium. It is worth noting that these conditions only show the non-monotonic relationship between the optimal lockdown and PHSI efficiency for FP nursing homes and do not apply to other sections throughout.

5.2 Data, calibration, and estimation of ι and θ

5.2.1 Data and calibration

To calibrate the two-sector N-SIRD model, we use data on nursing homes from several sources. Importantly, we collected the data to reflect the reality of nursing homes as much as possible during our study period (May 31 to August 16, 2020). Data on the economic variables come from the Bureau of Labor Statistics and the Senior Living Project. We use samples of nursing home networks collected by Chen et al. (2021). Using data from Google's Community Mobility Reports (CMR, 2020), we proxy the lockdown variable by the percentage change in U.S. workplace visits aggregated at the state level over our study period. The reports compile mobility data from visits to different categories of places, such as retail and recreation, groceries and pharmacies, parks, transit stations, workplaces, and residences. The mobility levels are then compared with each region's baseline (e.g., mean, median) during five weeks from January 3 to February 6, 2020. The Google Reports use the median level of the corresponding category as the baseline variable. Of the six categories, we choose workplace visits to capture the lockdown policy in our analysis since nursing homes are considered workplaces. For clarity, we summarize in Table B1 in Appendix B all relevant data sources.

5.2.2 Estimation of ι and θ

We use a simulated minimum distance estimator to estimate the COVID-19 PHSI profile (ι, θ) for 40 U.S. states. Formally, let us index a U.S. state by $s \in \overline{S}$, with $\overline{S} = \{1, ..., 40\}$. Let d_{ts} denote the number of COVID-19 deaths observed at time $t = 1, ..., T$ in the U.S. state $s \in \overline{S}$.[20] For each value of the PHSI profile (ι, θ), we can simulate death dynamics denoted as $\hat{d}_{ts}(\iota, \theta)$. For each U.S. state $s \in \overline{S}$, we estimate the PHSI profile (ι, θ) that we denote as $(\hat{\iota}_s, \hat{\theta}_s)$ by solving the following minimization problem:

$$(\hat{\iota}_s, \hat{\theta}_s) = argmin \left\{ \sum_{t=1}^{T} (\hat{d}_{ts}(\iota, \theta) - d_{ts})^2 \right\}, \ (\iota, \theta) \in [0, 1]^2. \tag{10}$$

[20] In line with Cronin and Evans (2022) and Fernández-Villaverde and Jones (2022), we use deaths as our main dependent variable instead of cases because deaths are subject to fewer measurement errors.

Existing literature on simulated minimum distance estimators (Forneron & Ng, 2018; Gertler & Waldman, 1992) suggests that $(\hat{\iota}_s, \hat{\theta}_s)$ is a consistent estimator of the profile (ι_s, θ_s) for the U.S. state $s \in \overline{S}$. From the estimated values of PHSI efficiency, $\hat{\theta}$, that we provide in Figure 2, the average PHSI efficiency level is 0.53 with a standard deviation of 0.38. The minimum PHSI efficiency level is 2.93×10^{-11} in South Dakota, and the maximum PHSI efficiency level is 0.973 in New York. We also plot in Figure 3 the estimated values of the COVID-19 tolerable infection incidence (ι). The average COVID-19 tolerable infection incidence level is 0.33, with a standard deviation of 0.22. The value of $\hat{\iota}$ is minimal in Connecticut (2.09×10^{-9}) and maximal in New Hampshire (0.657).

Figures 2 and 3 about here

Figure 4 represents the relationship between COVID-19 deaths and our estimated measure of the PHSI index—the PHSI efficiency $\hat{\theta}$. We observe the same pattern as in Section 3 when we used the OxCGRT indexes to measure the public and health safety measures implemented during the COVID-19 pandemic. As the number of deaths increases, policymakers are induced to impose stricter and more intense PHSI measures, which, with compliance and time, result in fewer fatalities. We can also note that the COVID-19 death gap between FP and NFP tends to increase with the PHSI efficiency quartile, confirming the significant role of government responses in explaining the differential death gap with ownership structures in U.S. nursing homes.

Figure 4 about here

The results in Table 4 show that the PHSI efficiency parameter $\hat{\theta}$ is positively and significantly correlated with all the OxCGRT (or PHSI) indexes. Additionally, while the tolerable infection incidence $\hat{\iota}$ is positively correlated with SI and ESI, it is negatively correlated with GRI and CHI, and all these correlations are insignificant. We should note that removing $\hat{\theta}$ as controls in Table 4 overturns the non-significance of $\hat{\iota}$ with all the OxCGRT indexes. The latter shows that PHSI efficiency $\hat{\theta}$ captures all the explanatory power of the tolerable infection incidence $\hat{\iota}$ in explaining government responses during the pandemic. Table 4 shows that higher values of tolerable infection incidence during the pandemic resulted from government financial support and stringent containment policies. As we may expect, a lower tolerable infection incidence induces higher mobility to workplaces since the correlation between $\hat{\iota}$ and the mobility variable is negative and significant. Similarly, effective lockdown policies are likely to reduce visits to workplaces. The latter explains the negative association of $\hat{\theta}$ and mobility during our study period.

Table 4 about here

5.3 PHSI efficiency and death differential in nursing homes: a regression-based analysis

In Section 4, we develop a model that combines epidemiology and economics to contribute to the literature that aims to explain the COVID-19 death gap observed between for-profits and not-for-profit nursing facilities.[21] In this section, we empirically evaluate the causal interplay between ownership structures, governmental interventions, and pandemic outcomes by estimating the effects of PHSI efficiency levels on COVID-19 deaths in nursing homes across 40 U.S. states and how these potential effects vary between FP and NFP nursing facilities. We use the following econometric equation:

$$\begin{aligned} \text{covid\_death}_{ijs} &= d_0\theta_s + a_1\text{Eig\_Cent}_{ijs} + a_2\text{County\_ses}_{js} \\ &+ a_3\text{D\_Profit}_{ijs} + a_4\text{Workplaces}_s \\ &+ d_1\theta_s \times \text{Eig\_Cent}_{ijs} + d_2\theta_s \times \text{County\_ses}_{js} \\ &+ d_3\theta_s \times \text{D\_Profit}_{ijs} + d_4\theta_s \times \text{Workplaces}_s \\ &+ c'X_{ijs} + F_j + \varepsilon_{ijs}, \end{aligned} \tag{11}$$

where covid_death_{ijs} is a variable counting the total number of COVID-19 deaths among residents in the nursing home i located in county j and state s; θ_s is the PHSI efficiency level in U.S. state s; Eig_Cent_{ijs} is the eigenvector centrality index of nursing home i; County_ses_{js} is county j's average socio-economic status; D_Profit_{ijs} is an indicator for whether a nursing home i is FP (1 if FP, and 0 if NFP); Workplaces_s is the average percentage change in workplace visits relative to a pre-pandemic level in state s; X_{ijs} represents other exogenous characteristics of the nursing home including the constant; F_j is the county fixed effect. Hence, in addition to estimating the effect of the interaction between PHSI efficiency and the FP status of a nursing home, we estimate how PHSI efficiency interacts with two other characteristics of a nursing home, including the eigenvector centrality index and the county's SES.

Table 5 about here

5.3.1 PHSI efficiency and COVID-19 deaths

Table 5 presents results from estimating variants of equation (11). In column 1, we regress the number of COVID-19 deaths on the ownership status of a nursing home. On average, the number of deaths in FP nursing homes is 19 percent higher relative to the mean than the number of deaths in NFP nursing homes. This difference is highly statistically significant. Column 2 additionally controls for PHSI efficiency, a nursing home's eigenvector centrality index, mobility (visits to workplaces), nursing home's overall quality rating, state's governor approval rate, state's stringency index, county's socioeconomic status, and the interaction term between PHSI efficiency levels and mobility. We find that the difference in the number of deaths between FP and NFP nursing homes decreases significantly and loses statistical significance, which implies that the control variables explain the difference found in column 1. Estimates from column 2 also imply that increased PHSI efficiency level decreases COVID-19 deaths in U.S. nursing homes. The estimated effect suggests that a one standard deviation increase in PHSI efficiency level reduces the number of deaths by

[21] For a brief survey on recent literature explaining this mortality gap, we refer interested readers to Bach-Mortensen et al. (2021).

around 5. Including additional controls in columns 3-6 has only a minimal effect on $\hat{\theta}$, the coefficients of $\hat{\theta}$ remain statistically indistinguishable from the estimate presented in column 2. Visits to workplaces reduce COVID-19 mortality, although the effect is not statistically significant. However, the estimate of the interaction term between $\hat{\theta}$ and "Workplaces" visits indicates that the total effect of PHSIs through reducing mobility on COVID-19 deaths depends on the PHSI efficiency parameter θ.

The specification presented in column 3 controls for the variables in column 2 and an interaction term between PHSI efficiency and the ownership status of a nursing home. Our findings show that the coefficient of the interaction term is positive and highly significant. The estimate suggests that relative to a situation in which the PHSI is inefficient, following a fully efficient PHSI, the death differential between FP and NFP nursing homes increases by 0.861, representing around 40 percent of the mean deaths. A one standard deviation increase in PHSI efficiency level raises the death gap between FP and NFP nursing homes by over 15 percent relative to the mean. Including additional controls in column 6 (the full specification) increases the size of this effect. The result in column 6 suggests that moving from a totally inefficient PHSI to a fully efficient PHSI raises the death differential between FP and NFP nursing homes by around 60 percent relative to the mean. These effects are large and statistically significant.

The results in columns 2 to 6 also suggest that nursing homes with more central network positions (i.e., nursing homes with higher eigenvector centrality) experience higher COVID-19 mortality. The interaction between PHSI efficiency levels and the eigenvector centrality index in the specification presented in column 4 shows that the death count gap between more central nursing homes and those less central increases with PHSI efficiency. The regression results reported in columns 2 to 6 suggest a consistently negative and significant direct effect of the county's wealth status on COVID-19 deaths. In particular, when controlling for all characteristics in column 6, the gap between poorer and richer counties in COVID-19 deaths reduces as the lockdown policies become more effective.

In the specification reported in columns 2 to 6 in Table 5, we control an additional set of variables, including the overall rating of a nursing home, the governor's approval rating, and the state's stringency index. Including these variables does not affect the validity of the relationship between our outcome of interest and the main variables discussed above. Our regression results are also robust when controlling for other government pandemic mitigation measures captured by the PHSI (or OxCGRT) indexes; we report the findings of these specifications in Appendix B. Overall, our analysis implies that the effects of government policy response to health crises significantly differ for FP and NFP nursing homes. These effects also differ along with other nursing home characteristics, such as network centrality and county SES.

5.3.2 Possible Mechanisms and Policy Implications

The findings presented in the previous sections reveal the contribution of PHSIs to explaining the COVID-19 death gap observed between FP and NFP nursing homes during the pandemic. In this section, we propose some mechanisms through which changes in PHSI efficiency levels could have relatively benefited NFP over FP nursing homes in managing the COVID-19 pandemic. Table 6 suggests that an increase in PHSI efficiency levels has reduced the occurrence of PHSI rule violations in nursing homes. It has also led to more shortages of both aid and nursing staff. However, the

availability of clinical staff and other staff was not significantly affected. FP nursing homes are more likely to be central in the network and experience marginally less shortage of nursing staff. As the PHSI efficiency level increases, FP nursing homes are more likely to register rule violations than NFP nursing homes. They also experience a more severe shortage of nursing staff.

Table 6 about here

As the tolerable infection incidence level decreases, policymakers are unlikely to accept more infections and exert more pressure to reduce individual mobility. Coupled with the high demand for nurses during the COVID-19 pandemic, higher PHSIs led to the reduction of the use of part-time and unskilled nursing and aid staff. If FP nursing homes were heavily relying on part-time nurses, they would suffer the most COVID-19 fatalities since the nurse shortage gap generated by the PHSIs would produce more deaths in FP nursing homes compared to others. Moreover, FPs, with a more acute nursing staff shortage, may not be able to well manage or comply with all specifications of new PHSIs as NFP homes. Thus, we could observe more violations of PHSIs in FPs relative to NFPs. These rule violations, coupled with the lower overall quality and a higher level of centrality, could imply more pandemic fatalities in FP nursing facilities.

Labor and infrastructure are some of the most significant cost entries of care providers in the long-term care sector. Generally, care providers devise strategic management plans for these inputs to stay afloat or maximize returns, as in the case of for-profit nursing facilities. The response of policymakers to the COVID-19 pandemic was marked by the rapid adoption and implementation of several PHSIs. The long-term care sector was considered an essential sector during this health crisis, meaning that nursing staff could provide their services to nursing homes during lockdown periods. However, the literature documents that for-profit nursing homes tend to allocate fewer resources toward skilled nursing staff, which, in addition to other safety and preventive personnel equipment, are essential factors in fighting pandemics. Thus, without proper enforcement and incentive policies, nursing care facilities may not appropriately use the financial support from governments. The latter holds true even if there are insurance products in the long-term care sectors that may provide financial support to care providers during pandemics like COVID-19. Hence, social planners should consider the presence of information asymmetry and moral hazard behaviors when implementing PHSI strategies during pandemics. Addressing this issue is a question of interest, but it is beyond the scope of the current paper.

Our analyses reveal that in a pandemic, government policies to reduce the contagion and save lives can affect economic agents differently depending on other incentives they face. Our findings shed light on the role that PHSIs may have played in the differential in COVID-19 deaths between FP and NFP U.S. nursing homes. Exploring transmission mechanisms points to a potential moral hazard problem in nursing care facilities or resource constraints.

6 Concluding Remarks

This study examines how the efficiency of government policy response is affected by market structure during a pandemic. It does so by analyzing the potential effects of public health and safety interventions (PHSIs) on for-profit (FP) and not-for-profit

(NFP) organizations, with a focus on the long-term care market in the United States during the COVID-19 pandemic. We find that for-profit (FP) nursing homes have higher death rates than not-for-profit (NFP) ones. Moreover, this gap increases with the stringency of PHSIs. Factors like nursing home quality and county socioeconomic status moderate the impact of ownership on death rates.

To gain a better understanding of the causal links and explore possible mechanisms, we introduce a two-sector, continuous-time theoretical model combining economic principles and epidemiology to address this problem. Without an effective cure or vaccine, the planner seeks a PHSI strategy to curb the spread of the contagion, which spreads among agents through physical contact. Notably, the planner's decision depends on their tolerable infection incidence (ι)—preference for enforcing a stringent containment strategy—, the nature of the pandemic, and the state of the economy. Although PHSI strategy can reduce the spread of infection and save lives, its unintended consequences could adversely affect the economy and the flow of movements in the population, resulting in high social and economic costs. Using lockdown as a control variable, we use tools from optimal control theory to solve this dilemma. Our analysis reveals that each feasible solution to the planner's problem depends on the efficiency of PHSI strategies, i.e., how these interventions effectively reduce the contagion, the infection incidence level tolerated by the planner, the prevailing network of physical contacts in the economy, and exogenous epidemiological parameters.

We apply our model to the long-term care sector in the U.S. Providers in this market can be differentiated by ownership type (for-profit, not-for-profit, and public providers). Using unique data on U.S. nursing home networks and other data sources, we calibrate our mean-field network-based theoretical model and jointly estimate the PHSI efficiency parameter (θ) and the tolerable COVID-19 infection incidence level (ι) for 40 U.S. states. Our estimated values show significant variations in these variables across U.S. states. Our regression-based estimations show that for-profit nursing homes experience a higher death rate than not-for-profit nursing homes and that this death differential increases with PHSI efficiency. A one-standard-deviation increase in PHSI efficiency level raises the mortality gap between for-profit and not-for-profit nursing homes by 23 percent relative to the mean. In general, the analysis shows that the effects of government policy responses to health crises vary significantly depending on the characteristics of the nursing home.

Our analyses imply that the structure of markets and their heterogeneity in experiencing uncertain shocks can help policymakers design optimal interventions for future pandemics. While improved safety measures undoubtedly reduce rule violations, they also exacerbate staff and resource shortages, particularly affecting FP nursing homes. Lockdowns further compound this issue by making it increasingly difficult to recruit sufficient nursing staff, especially for facilities that rely on part-time workers. This scarcity of nurses may contribute to higher mortality rates in FP nursing homes as they struggle to maintain safety standards and adhere to regulations. In addition, FP nursing homes face additional challenges due to a lack of insurance coverage during pandemics such as COVID-19, which could hinder their ability to respond effectively to increased demand. As PHSI efficiency increases, FP nursing homes become more central in social networks than NFP nursing homes, indicating difficulties to comply with lockdown measures among the former. To improve overall

safety, targeted monitoring strategies are recommended for better rule implementation. Furthermore, addressing the incomplete insurance market for FP homes in pandemic resource allocations is vital, although the methodology for such allocation is beyond the scope of this paper.

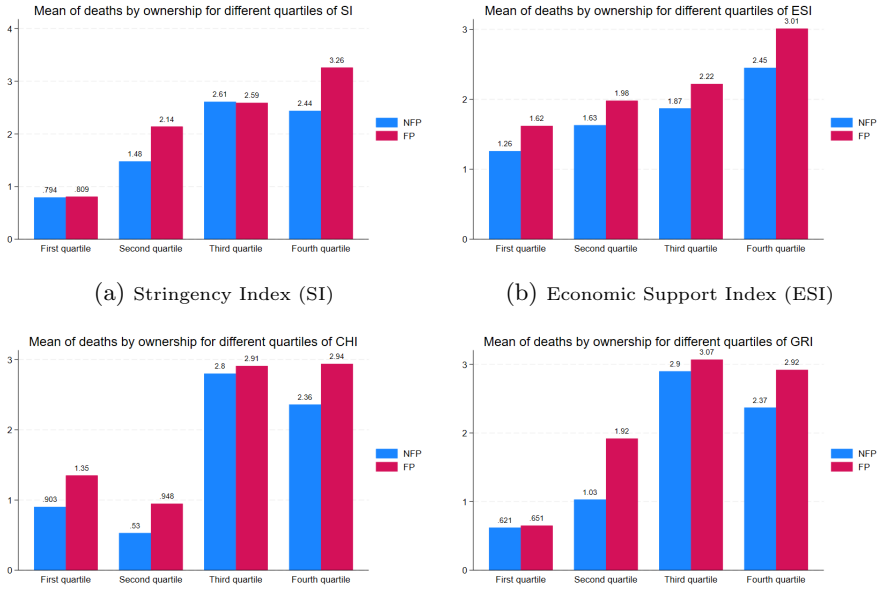

(a) Stringency Index (SI)

(b) Economic Support Index (ESI)

(c) Containment Health Index (CHI)

(d) Government Response Index (GRI)

Fig. 1: FP vs NFP COVID-19 death Gap by Quartile of PHSI Indexes. Notes: Data are from CMS as of 31 May 2020 and the COVID STATES PROJECT.

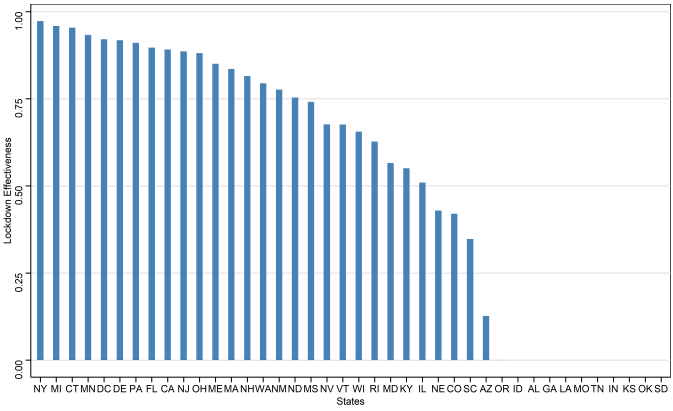

Fig. 2: PHSI efficiency levels across U.S. state (θ). Notes: The parameter θ estimates the effectiveness of the U.S. state governor's PHSIs (lockdown policies) from May 31 to August 16, 2020. Using the CMS data and the calibrated parameters in the model, we estimate θ for 40 U.S. states. The average value of estimates is 0.53, and the standard deviation is 0.38.

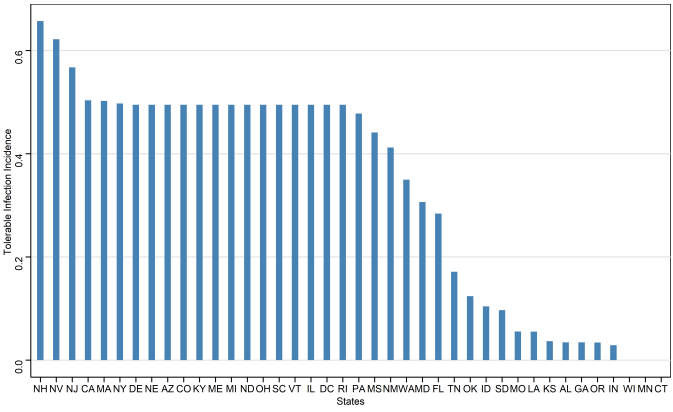

Fig. 3: Tolerable infection incidence across U.S. states (ι). Notes: The parameter ι estimates the tolerable COVID-19 infection incidence of the U.S. state governor from May 31 to August 16, 2020. Using the CMS data and the calibrated parameters in the model, we estimate ι for 40 U.S. states. The average value of estimates is 0.33, and the standard deviation is 0.22.

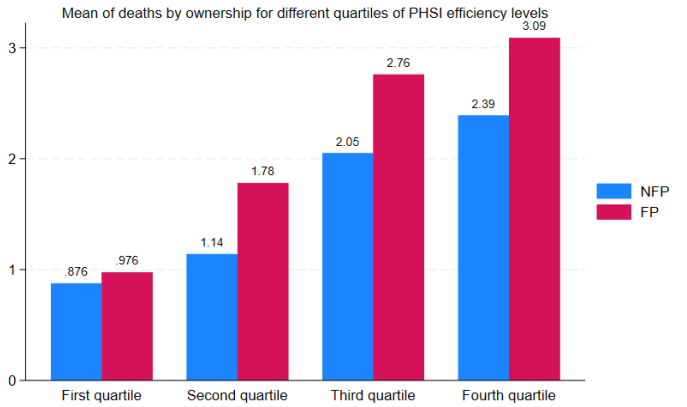

Fig. 4: FP vs NFP COVID-19 death Gap by Quartile of PHSI efficiency levels. Notes: Data are from CMS as of May 31, 2020, and authors' estimations.

Table 1: Descriptive statistics of U.S. nursing homes and U.S. states data

Nursing Homes							
	All			FP		NFP	
	Mean	SD	Count	Mean	Count	Mean	Count
Variables							
Urban	0.74	0.44		0.77		0.68	
Beds	107.16	61.65		110.22		100.25	
Beds occupied	78.9	50.77		80.68		74.88	
CMS quality rating (1-5)	3.76	1.22		3.69		3.94	
Overall rating	3.24	1.41		3.02		3.74	
COVID-19 deaths	2.17	6.49		2.33		1.80	
Home eigenvector centrality	0.09	0.18		0.09		0.06	
Number of nursing homes			11395		7895		3500

U.S. states (40 states)		
	Mean	SD
Variables		
Republican Governor	0.48	
Female Governor	0.2	
South	0.28	
Governor Approval	56.11	9.3
GDP Growth	-3.51	1.36
County SES	404.42	276.84
Visits to workplaces	-28.46	4.78
Stringency Index	63.25	8.80
Government Response Index	61.87	7.66
Containment Health Index	60.92	7.41
Economic Support Index	68.55	14.42

Notes: Data are from the CMS as of May 31, 2020, Chen et al. (2021), Hale et al. (2021), Google's Community Mobility Reports (CMR, 2020), and the COVID STATES PROJECT. Binary variables are a percent of nursing homes; continuous variables are mean values, with standard deviations in parentheses.

Table 2: Effects of policy response indexes on COVID-19 deaths in U.S. nursing homes

	(1)	(2)	(3)	(4)	(5)
For-profit_ind	0.414***	-1.289	-0.529	-0.220	-1.598
	(3.31)	(-1.15)	(-0.47)	(-0.20)	(-1.47)
Stringency_Index		-0.407***			
		(-3.71)			
Government_Response_Index			-0.507***		
			(-5.75)		
Containment_Health_Index				-0.670***	
				(-7.22)	
Economic_Support_Index					-0.00467
					(-0.10)
Eigenvector_weeks_1_11		3.334***	3.442***	3.473***	3.405***
		(7.47)	(7.72)	(7.79)	(7.63)
Workplaces		0.752***	1.030***	1.389***	-0.181
		(2.78)	(5.00)	(6.49)	(-1.53)
Overall_rating		-0.199***	-0.197***	-0.195***	-0.195***
		(-4.58)	(-4.55)	(-4.49)	(-4.52)
County_ssa		0.00771***	0.00625***	0.00636***	0.00767***
		(7.27)	(6.18)	(6.17)	(7.58)
Prof_workplace		-0.0497	-0.0209	-0.0100	-0.0604
		(-1.18)	(-0.49)	(-0.24)	(-1.46)
SI_workplace		-0.0159***			
		(-3.69)			
GRI_workplace			-0.0205***		
			(-5.98)		
CHI_workplace				-0.0268***	
				(-7.39)	
ESI_workplace					-0.000757
					(-0.44)
Constant	2.714***	20.52***	26.51***	35.68***	-3.905
	(6.60)	(3.06)	(5.16)	(6.69)	(-1.28)
Observations	11546	11418	11418	11418	11418
R^2	0.042	0.087	0.091	0.093	0.086

t statistics in parentheses

* $p < 0.10$, ** $p < 0.05$, *** $p < 0.01$

Notes: Data are from the CMS as of May 31, 2020, Chen et al. (2021), Hale et al. (2021), Google's Community Mobility Reports (CMR, 2020), and authors' estimations. The dependent variable is the number of COVID-19 deaths among residents in a nursing home. t statistics in parentheses. $^{*}p < 0.1$, $^{**}p < 0.05$, $^{***}p < 0.01$.

Table 3: Oaxaca-Blinder Decomposition of COVID-19 Death Gap FP vs NFP

	(1)	(2)	(3)	(4)
Overall				
NFP	1.803***	1.803***	1.803***	1.803***
	(17.70)	(17.70)	(17.70)	(17.69)
FP	2.327***	2.327***	2.327***	2.327***
	(31.04)	(31.04)	(31.04)	(31.03)
Difference	-0.524***	-0.524***	-0.524***	-0.524***
	(-4.14)	(-4.14)	(-4.14)	(-4.14)
Explained	-0.453***	-0.503***	-0.507***	-0.522***
	(-6.56)	(-7.19)	(-7.17)	(-7.20)
Unexplained	-0.0715	-0.0207	-0.0176	-0.00215
	(-0.52)	(-0.15)	(-0.13)	(-0.02)
Explained				
Stringency Index	-0.00970			0.201***
	(-0.49)			(4.27)
Eig_Cent	-0.150***	-0.155***	-0.154***	-0.153***
	(-5.83)	(-5.93)	(-5.91)	(-5.92)
Workplaces	-0.130***	-0.101***	-0.106***	-0.122***
	(-5.03)	(-4.55)	(-4.70)	(-4.89)
Overall_rating	-0.143**	-0.137**	-0.139**	-0.130**
	(-2.56)	(-2.45)	(-2.49)	(-2.34)
County_ssa	-0.0200**	-0.0202**	-0.0199**	-0.0184**
	(-2.17)	(-2.19)	(-2.17)	(-2.06)
Government Response Index		-0.0916***		-0.249***
		(-3.66)		(-2.78)
Containment HealthIndex			-0.0879***	-0.0501
			(-3.23)	(-0.48)
Unexplained				
Stringency Index	-0.464			-4.346
	(-0.35)			(-1.64)
Eig_Cent	0.162**	0.172**	0.170**	0.166**
	(2.30)	(2.44)	(2.41)	(2.37)
Workplaces	-2.657**	-3.064**	-3.166**	-1.484
	(-2.05)	(-2.35)	(-2.49)	(-1.11)
Overall_rating	-0.0539	-0.0262	-0.0335	0.0113
	(-0.19)	(-0.09)	(-0.12)	(0.04)
County_ssa	-0.329*	-0.321*	-0.327*	-0.263
	(-1.89)	(-1.85)	(-1.88)	(-1.51)
Government Response Index		0.733		0.444
		(0.53)		(0.08)
Containment Health Index			0.620	3.433
			(0.44)	(0.61)
Constant	3.270**	2.486*	2.719**	2.036
	(2.54)	(1.90)	(2.02)	(1.49)
Observations	11419	11419	11419	11419

t statistics in parentheses

* $p < 0.10$, ** $p < 0.05$, *** $p < 0.01$

Notes: Data are from the CMS as of May 31, 2020, Chen et al. (2021), Hale et al. (2021), Google's Community Mobility Reports (CMR, 2020), and authors' estimations. The dependent variable is the number of COVID-19 deaths among residents in a nursing home. t statistics in parentheses. $^*p < 0.1$, $^{**}p < 0.05$, $^{***}p < 0.01$.

Table 4: Correlation between $\hat{\theta}$, $\hat{\iota}$, visits to workplaces and OxCGRT (PHSI) indexes

	Visits to Workplaces	Stringency Index	Government Response Index	Containment Health Index	Economic Support Index
$\hat{\theta}$	-5.56 ***	12.11***	11.09***	10.70***	13.85***
	(-22.30)	(23.52)	(26.06)	(25.97)	(11.97)
$\hat{\iota}$	-1.54 ***	0.933	-0.115	-0.569	3.083
	(-3.55)	(1.05)	(-0.16)	(-0.80)	(1.54)
Constant	-24.99 ***	56.50 ***	56.01***	55.42***	60.16***
	(-174.07)	(190.78)	(228.78)	(233.87)	(90.37)
Observations	3120	3120	3120	3120	3120
R^2	0.236	0.229	0.256	0.249	0.079

Notes: Data are from Hale et al. (2021), Google's Community Mobility Reports (CMR, 2020), and authors' estimations. t statistics in parentheses. * $p < 0.1$, ** $p < 0.05$, *** $p < 0.01$.

Table 5: Effects of PHSI efficiency on COVID-19 deaths in U.S. nursing homes

	(1)	(2)	(3)	(4)	(5)	(6)
D_Profit	0.414***	0.146	-0.221	0.156	0.140	-0.425***
	(3.31)	(1.11)	(-1.38)	(1.19)	(1.05)	(-2.65)
$\hat{\theta}$		-12.03***	-11.40***	-11.85***	-12.26***	-12.12***
		(-6.83)	(-6.43)	(-6.74)	(-6.71)	(-6.64)
Eig_Cent		3.605***	3.615***	2.357***	3.600***	2.428***
		(7.99)	(8.01)	(3.80)	(7.97)	(3.88)
Workplaces		0.0498	0.0612	0.0523	0.0492	0.0660
		(1.09)	(1.32)	(1.15)	(1.08)	(1.43)
Overall Rating		-0.193***	-0.191***	-0.191***	-0.193***	-0.191***
		(-4.42)	(-4.38)	(-4.39)	(-4.43)	(-4.39)
Governor Approval		0.0684***	0.0655***	0.0661***	0.0691***	0.0657***
		(9.97)	(9.43)	(9.55)	(9.92)	(9.38)
Stringency_Index		0.00422	0.0130	0.00741	0.00223	0.00992
		(0.43)	(1.26)	(0.75)	(0.22)	(0.96)
County_ses		0.00574***	0.00559***	0.00563***	0.00592***	0.00641***
		(5.33)	(5.18)	(5.25)	(5.22)	(5.72)
$\hat{\theta}\times$ Workplaces		-0.450***	-0.429***	-0.444***	-0.458***	-0.455***
		(-6.91)	(-6.59)	(-6.83)	(-6.84)	(-6.81)
$\hat{\theta}\times$ D_Profit			0.861***			1.287***
			(2.75)			(4.19)
$\hat{\theta}\times$ Eig_Cent				2.713**		2.528**
				(2.27)		(2.09)
$\hat{\theta}\times$ County_ses					-0.000354	-0.00185***
					(-0.71)	(-4.09)
Constant	2.714***	-0.977	-1.083	-0.993	-0.910	-0.800
	(6.60)	(-0.91)	(-1.01)	(-0.92)	(-0.85)	(-0.74)
Observations	11546	11406	11406	11406	11406	11406
R^2	0.042	0.095	0.096	0.095	0.095	0.096

Notes: Data are from the CMS as of May 31, 2020, Chen et al. (2021), Hale et al. (2021), Google's Community Mobility Reports (CMR, 2020), and authors' estimations. The dependent variable is the number of COVID-19 deaths among residents in a nursing home. We provide in Table B2 some robustness checks of Table 5 with other OxCGRT indexes. t statistics in parentheses. $^{*}p < 0.1$, $^{**}p < 0.05$, $^{***}p < 0.01$.

Table 6: Effects of PHSI efficiency on Nursing Home Centrality, Rules violations, and Staff Shortages.

	(1)	(2)	(3)	(4)	(5)	(6)
D_Profit	0.0303***	-0.00366	-0.00498	-0.0194*	0.00219	-0.00502
	(6.49)	(-0.30)	(-0.42)	(-1.72)	(0.44)	(-0.54)
θ	0.00380	-0.675***	0.418***	0.189*	-0.0542	-0.129
	(0.07)	(-5.34)	(3.53)	(1.66)	(-1.25)	(-1.35)
Workplaces	-0.00684***	0.0188***	-0.00689**	-0.00173	0.00104	0.00274
	(-4.69)	(5.25)	(-2.13)	(-0.56)	(0.91)	(1.03)
Overall Rating	-0.00377***	-0.0791***	-0.0221***	-0.0230***	-0.00270**	-0.0110***
	(-3.20)	(-29.88)	(-8.32)	(-9.11)	(-2.34)	(-5.39)
Governor Approval	-0.000272	-0.00260***	0.00249***	0.00232***	0.000105	0.00111***
	(-1.23)	(-4.68)	(4.75)	(4.66)	(0.51)	(2.87)
County_ses	-0.0000605**	-0.0000451	-0.000110	-0.0000219	0.0000163	-0.0000539
	(-2.21)	(-0.71)	(-1.60)	(-0.34)	(0.57)	(-1.04)
$\theta\times$ Workplace	0.00170	-0.0294***	0.0166***	0.00838**	-0.00213	-0.00400
	(0.88)	(-6.18)	(3.73)	(1.97)	(-1.31)	(-1.12)
$\theta\times$ D_Profit	-0.0135	0.0928***	0.0288	0.0346*	0.00329	0.00649
	(-1.62)	(4.89)	(1.37)	(1.73)	(0.37)	(0.39)
Constant	-0.0765*	1.538***	-0.0852	0.0597	0.0469	0.131*
	(-1.88)	(15.83)	(-0.96)	(0.69)	(1.45)	(1.81)
Observations	12208	12208	11211	11211	11211	11211
R^2	0.080	0.112	0.044	0.042	0.019	0.036

t statistics in parentheses

* $p < 0.10$, ** $p < 0.05$, *** $p < 0.01$

Notes: Data are from the CMS as of May 31, 2020, Chen et al. (2021), Hale et al. (2021), Google's Community Mobility Reports (CMR, 2020), and authors' estimations. The dependent variables are (1) eigenvalue centrality, (2) violations, (3) aid shortage, (4) nursing staff shortage, (5) clinical staff shortage, and (6) other staff shortage. t statistics in parentheses. $^{*}p < 0.1$, $^{**}p < 0.05$, $^{***}p < 0.01$.

Appendix A Proof of theoretical results

A.1 Proof of Proposition 1

Given that $s_i = 1 - x_i - r_i - d_i$, for each $i \in N$, we can rewrite (ODE) as:

$$(\text{ODE}): \begin{cases} \dot{s_i} = -\beta(1 - x_i - r_i - d_i)(1 - \theta l_i) \sum\limits_{j \in N} [\mathcal{M}_{ij}(1 - \theta l_j)x_j] \\ \dot{x_i} = \beta(1 - x_i - r_i - d_i)(1 - \theta l_i) \sum\limits_{j \in N} [\mathcal{M}_{ij}(1 - \theta l_j)x_j] - (\gamma + \kappa)x_i \\ \dot{r_i} = \gamma x_i \\ \dot{d_i} = \kappa x_i. \end{cases}$$

Consider $F_i(t, X_i) = (F_{i1}(t, X_i), F_{i2}(t, X_i), F_{i3}(t, X_i), F_{i4}(t, X_i))^T$, a vector-valued function, where

$$\begin{aligned} F_{i1}(t, X_i) &= \beta(1 - x_i - r_i - d_i)(1 - \theta l_i) \sum_{j \in N} [\mathcal{M}_{ij}(1 - \theta l_j)x_j] - (\gamma + \kappa)x_i \\ F_{i2}(t, X_i) &= -\beta(1 - x_i - r_i - d_i)(1 - \theta l_i) \sum_{j \in N} [\mathcal{M}_{ij}(1 - \theta l_j)x_j] \\ F_{i3}(t, X_i) &= \gamma x_i \text{ and} \\ F_{i4}(t, X_i) &= \kappa x_i. \end{aligned}$$

The function F_{ik} is a continuously differentiable function, for each $i \in N$ and $k \in \{1, 2, 3, 4\}$. Consequently, the ODE admits a unique solution thanks to the theorem of existence and uniqueness of a solution for first-order general ordinary differential equations, where $l = (l_i)_{i \in N} \in [0, 1]^n$ is a vector of individual lockdown probabilities.

A.2 Existence of solutions for the planning problem

For simplicity, and in line with our application to the long-term care market, we assume that $\underline{\Pi}^A = -\overline{\Pi}^A = -\infty$, and $\underline{\Pi}^B = \overline{\Pi}^B = 0$. A general proof follows a similar reasoning. In (6), we also denote

$$f_i(x_i, r_i, d_i, l_i) = \beta(1 - x_i - r_i - d_i)(1 - \theta l_i) \sum_{j \in N} \mathcal{M}_{ij}(1 - \theta l_j)x_j - (\gamma + \kappa)x_i.$$

Then, $\dot{x_i} = f_i$. We assume that the control function $l_i : t \longrightarrow l_i(t) \in [0, 1]$ is continuous (or piecewise-continuous) and differentiable. Given that the function Π_i is concave, it follows that Π_i and the objective function, $e^{-\delta t}\mathcal{S}(k, x, r, d, l)$ in (6) are continuous and differentiable functions of their variables. Moreover, f_i and the right-hand sides of the laws of motion in (6) are all continuous and differentiable. The current Hamiltonian of the planner's problem in the system (6) is:

$$\mathcal{H}_c(l, x, r, d, \mu^1, \mu^2, \mu^3) = \sum_{i \in N^A} \Pi_i(k_i, h_i) + \sum_{i \in N} \mu_i^1 f_i + \sum_{i \in N} \mu_i^2 \gamma x_i + \sum_{i \in N} \mu_i^3 \kappa x_i,$$

where μ_i^j $(j = 1, 2, 3)$, for each $i \in N$, are costate variables. Given the constraints $\dot{x_i} \leq \iota$, $l_i(t) \in [0, 1]$ for all $i \in N$, and $\Pi_i(k_i, h_i) = 0$, for all $i \in N^B$, we can augment the current Hamiltonian $\mathcal{H}_c$ into the current Lagrangian function:

$$\mathcal{L}_c(l,x,r,d,\mu^1,\mu^2,\mu^3,\eta^1,\eta^2,\eta^3,\eta^4) = \sum_{i\in N^A}\Pi_i(k_i,h_i) + \sum_{i\in N}\mu_i^1 f_i + \sum_{i\in N}\mu_i^2\gamma x_i$$
$$+ \sum_{i\in N}\mu_i^3\kappa x_i + \sum_{i\in N}\eta_i^1(\iota - f_i) + \sum_{i\in N}\eta_i^2 l_i + \sum_{i\in N}\eta_i^3(1-l_i) + \sum_{i\in N^B}\eta_i^4\Pi_i(k_i,h_i)$$

where the parameters η^j, $j = 1,2,3,4$, are Lagrange multipliers. For any subset O of N, let $\mathbf{1}_O$ be the function defined on N by

$$\mathbf{1}_O(i) = \begin{cases} 1 & \text{if } i \in O \\ 0 & \text{if otherwise.} \end{cases}$$

We can rewrite $\mathcal{L}_c$ as:

$$\mathcal{L}_c(l,x,r,d,\mu^1,\mu^2,\mu^3,\eta^1,\eta^2,\eta^3,\eta^4) = \sum_{i\in N}\left(\mathbf{1}_{N^A}(i) + \eta_i^4\left(1-\mathbf{1}_{N^A}(i)\right)\right)\Pi_i(k_i,h_i)$$
$$+ \sum_{i\in N}(\mu_i^1 - \eta_i^1)f_i + \sum_{i\in N}\mu_i^2\gamma x_i + \sum_{i\in N}\mu_i^3\kappa x_i + \iota\sum_{i\in N}\eta_i^1 + \sum_{i\in N}\eta_i^2 l_i + \sum_{i\in N}\eta_i^3\left(1-l_i\right) \tag{A1}$$

The first-order conditions for maximizing $\mathcal{L}_c$ call for, assuming interior solutions,

$$\frac{\partial\mathcal{L}_c}{\partial l_k} = 0,\ k \in N, \tag{A2}$$

as well as for each $k \in N$:

$$\frac{\partial\mathcal{L}_c}{\partial\eta_k^1} = \iota - \dot{x_k} \geq 0, \qquad \eta_k^1 \geq 0, \qquad \eta_k^1\frac{\partial\mathcal{L}_c}{\partial\eta_k^1} = \eta_k^1(\iota - \dot{x_k}) = 0, \tag{A3}$$

$$\frac{\partial\mathcal{L}_c}{\partial\eta_k^2} = l_k \geq 0, \qquad \eta_k^2 \geq 0, \qquad \eta_k^2\frac{\partial\mathcal{L}_c}{\partial\eta_k^2} = \eta_k^2 l_k = 0, \text{ and} \tag{A4}$$

$$\frac{\partial\mathcal{L}_c}{\partial\eta_k^3} = 1 - l_k \geq 0, \qquad \eta_k^3 \geq 0, \qquad \eta_k^3\frac{\partial\mathcal{L}_c}{\partial\eta_k^3} = \eta_k^3(1-l_k) = 0, \tag{A5}$$

and the break-even condition for NFP nursing homes:

$$\frac{\partial\mathcal{L}_c}{\partial\eta_i^4} = \Pi_i(k_i,h_i) = 0, \text{ for all } i \in N^B. \tag{A6}$$

Finally, the other maximum-principle conditions that include the dynamics for state and co-state variables are, for $k \in N$:

$$\dot{x_k} = \frac{\partial\mathcal{L}_c}{\partial\mu_k^1} \qquad \dot{r_k} = \frac{\partial\mathcal{L}_c}{\partial\mu_k^2} \qquad \dot{d_k} = \frac{\partial\mathcal{L}_c}{\partial\mu_k^3} \tag{A7}$$

$$\dot{\mu_k^1} = \delta\mu_k^1 - \frac{\partial\mathcal{L}_c}{\partial x_k} \qquad \dot{\mu_k^2} = \delta\mu_k^2 - \frac{\partial\mathcal{L}_c}{\partial r_k} \qquad \dot{\mu_k^3} = \delta\mu_k^3 - \frac{\partial\mathcal{L}_c}{\partial d_k} \tag{A8}$$

Let denote by $\{l^*(t)\}_t$ an optimal path of the control variable and an optimal path for state variables by $\{X_t^* = (x^*(t), r^*(t), d^*(t), s^*(t))\}_t$. We note that Eqs. (A2)–(A8) constitute a set of necessary conditions that characterize the optimal solution of the optimal control problem under an infinite time horizon. As it stands, Eqs. (A2) and (A8) do not allow us to solve the system of differential equations constituted by (A2)–(A8) since we only have an initial condition for X_t^*, namely $X^*(0) = X(0)$, and a complete solution of the system (6) requires two boundary conditions. Therefore, we

need to find another boundary condition. Generally, to obtain the complete solution of the optimal control under an infinite time horizon, the following conditions are required for the transversality condition at infinity:

$$\lim_{t\to\infty} \mu_k^1(t) \geq 0 \text{ and } \lim_{t\to\infty} \mu_k^1(t)x_k(t) = 0; \tag{A9}$$

$$\lim_{t\to\infty} \mu_k^2(t) \geq 0 \text{ and } \lim_{t\to\infty} \mu_k^2(t)r_k(t) = 0; \tag{A10}$$

$$\lim_{t\to\infty} \mu_k^3(t) \geq 0 \text{ and } \lim_{t\to\infty} \mu_k^3(t)d_k(t) = 0. \tag{A11}$$

Let denote

$$\mathcal{H}_c^{max}(x, r, d, \mu^1, \mu^2, \mu^3, t) = \max_l \mathcal{H}_c(l, x, r, d, \mu^1, \mu^2, \mu^3, t). \tag{A12}$$

By definition, each state variable x, r, or d is non-negative at each period t. Assume that given the list (μ^1, μ^2, μ^3) and t, the map $(x, r, d) \longrightarrow \mathcal{H}_c^{max}(x, r, d, \mu^1, \mu^2, \mu^3, t)$ is jointly concave in the variables (x, r, d). Then, if $\{l^*(t)\}_t$, $\{X_t^* = (x^*(t), r^*(t), d^*(t), s^*(t))\}_t$, and $\{(\mu^1(t), \mu^2(t), \mu^3(t))\}_t$ constitute a solution of the system comprised by (A2)–(A11). The lockdown profile $\{l^*(t)\}_t$ is the solution of the planner's problem in (6). In case the function $\mathcal{H}_c^{max}(x, r, d, \mu^1, \mu^2, \mu^3, t)$ is jointly strictly concave in the variables (x, r, d), then the optimal path $\{l^*(t)\}_t$ is unique.

A.3 Further derivations for simulations

In what follows, we extend the theoretical derivation of the planning problem, which proves useful in our simulations. Recall that

$$f_i(x_i, r_i, d_i, l_i) = \beta(1 - x_i - r_i - d_i)(1 - \theta l_i) \sum_{j\neq i} [\mathcal{M}_{ij}(1 - \theta l_j)x_j] - (\gamma + \kappa)x_i.$$

Then,

$$\frac{\partial f_i}{\partial l_k} = \begin{cases} -\beta\theta(1 - x_i - r_i - d_i) \sum\limits_{j\neq i} [\mathcal{M}_{ij}(1 - \theta l_j)x_j] & \text{if } k = i \\ -\beta\theta(1 - x_i - r_i - d_i)(1 - \theta l_i)\mathcal{M}_{ik}x_k & \text{if } k \neq i \end{cases}$$

$$\frac{\partial f_i}{\partial x_k} = \begin{cases} -\beta(1 - \theta l_i) \sum\limits_{j\neq i} [\mathcal{M}_{ij}(1 - \theta l_j)x_j] - (\gamma + \kappa) & \text{if } k = i \\ \beta(1 - x_i - r_i - d_i)(1 - \theta l_i)(1 - \theta l_k)\mathcal{M}_{ik} & \text{if } k \neq i \end{cases}$$

$$\frac{\partial f_i}{\partial r_k} = \frac{\partial f_i}{\partial d_k} = \begin{cases} -\beta(1 - \theta l_i) \sum\limits_{j\neq i} [\mathcal{M}_{ij}(1 - \theta l_j)x_j] & \text{if } k = i \\ 0 & \text{if } k \neq i. \end{cases}$$

We also recall that

$$\Pi_i(k_i, s_i, x_i, r_i, d_i, l_i) \equiv \Pi_i(k_i, x_i, r_i, d_i, l_i) = p_i y_i(k_i, x_i, r_i, d_i, l_i) - w_i h_i(x_i, r_i, d_i, l_i).$$

Therefore, for each i and k, and for each u in $\{x_k, r_k, d_k, l_k\}$, it holds that

$$\frac{\partial \Pi_i}{\partial u} = \begin{cases} p_i \frac{\partial y_i}{\partial u} - w_i \frac{\partial h_i}{\partial u} & \text{if } k = i \\ 0 & \text{if } k \neq i. \end{cases} \tag{A13}$$

For each $k \in N$, we can write $\frac{\partial \mathcal{L}_c}{\partial l_k}$ as:

$$\frac{\partial \mathcal{L}_c}{\partial l_k} = \sum_{i\in N} \left(\mathbf{1}_{N^A}(i) + \eta_i^4 \left(1 - \mathbf{1}_{N^A}(i)\right) \right) \frac{\partial \Pi_i}{\partial l_k} + \sum_{i\in N} (\mu_i^1 - \eta_i^1) \frac{\partial f_i}{\partial l_k} + \eta_k^2 - \eta_k^3$$

$$\overset{(A13)}{=} \left(\mathbf{1}_{N^A}(k) + \eta_k^4\left(1 - \mathbf{1}_{N^A}(k)\right)\right)\frac{\partial \Pi_k}{\partial l_k} + \sum_{i\in N}(\mu_i^1 - \eta_i^1)\frac{\partial f_i}{\partial l_k} + \eta_k^2 - \eta_k^3.$$

Hence, using the first-order conditions in Eq. (A2), Eq. (A13) becomes:

$$\left(\mathbf{1}_{N^A}(k) + \eta_k^4\left(1 - \mathbf{1}_{N^A}(k)\right)\right)\left(p_k\frac{\partial y_k}{\partial l_k} - w_k\frac{\partial h_k}{\partial l_k}\right) + \sum_{i\in N}(\mu_i^1 - \eta_i^1)\frac{\partial f_i}{\partial l_k} + \eta_k^2 - \eta_k^3 = 0. \tag{A14}$$

Continuing our analysis of the problem (6), we need to differentiate Eq. (A14) with respect to time t. Recall that for each $i \in N$, $k_i = k_i(t) = K$, for all t, $h_k = 1 - \theta l_k$, $k \in N$, and $y_k = K^\alpha(1-\theta l_k)^{1-\alpha}$, $k \in N$, $\alpha \in [0,1]$. Differentiating y_k and h_k with respect to l_k yield:

$$\frac{\partial y_k}{\partial l_k} = -(1-\alpha)\theta K^\alpha(1-\theta l_k)^{-\alpha} \text{ and } \frac{\partial h_k}{\partial l_k} = -\theta.$$

It follows that:

$$\frac{\partial^2 y_k}{\partial t \partial l_k} = -\alpha(1-\alpha)\theta^2 K^\alpha \dot{l_k}(1-\theta l_k)^{-\alpha-1} \text{ and } \frac{\partial^2 h_k}{\partial t \partial l_k} = 0.$$

For $k \neq i$, recall that $\frac{\partial f_i}{\partial l_k} = -\beta\theta(1 - x_i - r_i - d_i)(1-\theta l_i)\mathcal{M}_{ik}x_k$. Then,

$$\begin{aligned}\frac{\partial^2 f_i}{\partial t \partial l_k} &= \beta\theta(\dot{x}_i + \dot{r}_i + \dot{d}_i)(1-\theta l_i)\mathcal{M}_{ik}x_k + \beta\theta^2(1 - x_i - r_i - d_i)\dot{l_i}\mathcal{M}_{ik}x_k \\ &- \beta\theta\left(1 - x_i - r_i - d_i\right)(1-\theta l_i)\mathcal{M}_{ik}f_k.\end{aligned}$$

For $k = i$, we also have $\frac{\partial f_i}{\partial l_k} = -\beta\theta(1 - x_i - r_i - d_i)\sum_{j\neq i}[\mathcal{M}_{ij}(1-\theta l_j)x_j]$. Then,

$$\begin{aligned}\frac{\partial^2 f_i}{\partial t \partial l_i} &= \beta\theta(\dot{x}_i + \dot{r}_i + \dot{d}_i)\sum_{j\neq i}[\mathcal{M}_{ij}(1-\theta l_j)x_j] \\ &- \beta\theta\left(1 - x_i - r_i - d_i\right)\sum_{j\neq i}[(1-\theta l_j)f_j - \theta\dot{l_j}x_j]\mathcal{M}_{ij}.\end{aligned}$$

Differentiating Eq. (A14) with respect to time t, assuming that prices p and w are time-invariant yield:

$$E_1 + \beta\theta\sum_{i\in N}\left(\mu_i^1 - \eta_i^1\right)\left(\delta_{ik}E_2 + (1-\delta_{ik})\mathcal{M}_{ik}E_3\right) + E_4 = 0, \tag{A15}$$

where $\delta_{ik} = 1$ if $k = i$ and $\delta_{ik} = 0$ if $k \neq i$, and

$$E_1 = \left(\mathbf{1}_{N^A}(k) + \eta_k^4\left(1 - \mathbf{1}_{N^A}(k)\right)\right)\left(-\alpha(1-\alpha)\theta^2 p_k K^\alpha \dot{l_k}(1-\theta l_k)^{-\alpha-1}\right),$$

$$E_2 = \left(\dot{x}_i + \dot{r}_i + \dot{d}_i\right)\sum_{j\neq i}[\mathcal{M}_{ij}(1-\theta l_j)x_j] - (1 - x_i - r_i - d_i)\sum_{j\neq i}[(1-\theta l_j)\dot{x}_j - \theta\dot{l_j}x_j]\mathcal{M}_{ij},$$

$$E_3 = \left(\dot{x}_i + \dot{r}_i + \dot{d}_i\right)(1-\theta l_i)x_k + \theta(1 - x_i - r_i - d_i)\dot{l_i}x_k - (1 - x_i - r_i - d_i)\left(1-\theta l_i\right)\dot{x}_k,$$

$$E_4 = \sum_{i\in N}(\dot{\mu}_i^1 - \dot{\eta}_i^1)\frac{\partial f_i}{\partial l_k} + \dot{\eta}_k^2 - \dot{\eta}_k^3.$$

Using Eq. (A15), we obtain an expression of $\dot{l}_k$ as follow:

$$\dot{l}_k = \frac{1}{\overline{E}_1}\left[\beta\theta \sum_{i\in N}\left(\mu_i^1 - \eta_i^1\right)\left(\delta_{ik}E_2 + (1-\delta_{ik})\mathcal{M}_{ik}E_3\right) + E_4\right], \text{ where} \tag{A16}$$

$$\overline{E}_1 = \left(\mathbf{1}_{N^A}(k) + \eta_k^4\left(1 - \mathbf{1}_{N^A}(k)\right)\right)\left(\alpha(1-\alpha)\theta^2 p_k K^\alpha (1-\theta l_k)^{-\alpha-1}\right).$$

Using the other conditions from Eq. (A8) and using Eq. (A13), we obtain:

$$\begin{aligned}
\dot{\mu_k^1} &= \delta\mu_k^1 - \frac{\partial \mathcal{L}_c}{\partial x_k} \\
&= \delta\mu_k^1 - \left(\mathbf{1}_{N^A}(k) + \eta_k^4\left(1 - \mathbf{1}_{N^A}(k)\right)\right)\left(p_k\frac{\partial y_k}{\partial x_k} - w_k\frac{\partial h_k}{\partial x_k}\right) - \mu_k^2\gamma - \mu_k^3\kappa \\
&\quad - \sum_{i\in N}(\mu_i^1 - \eta_i^1)\frac{\partial f_i}{\partial x_k} \\
\dot{\mu_k^2} &= \delta\mu_k^2 - \frac{\partial \mathcal{L}_c}{\partial r_k} \\
&= \delta\mu_k^2 - \left(\mathbf{1}_{N^A}(k) + \eta_k^4\left(1 - \mathbf{1}_{N^A}(k)\right)\right)\left(p_k\frac{\partial y_k}{\partial r_k} - w_k\frac{\partial h_k}{\partial r_k}\right) - \sum_{i\in N}(\mu_i^1 - \eta_i^1)\frac{\partial f_i}{\partial r_k} \\
\dot{\mu_k^3} &= \delta\mu_k^3 - \frac{\partial \mathcal{L}_c}{\partial d_k} \\
&= \delta\mu_k^3 - \left(\mathbf{1}_{N^A}(k) + \eta_k^4\left(1 - \mathbf{1}_{N^A}(k)\right)\right)\left(p_k\frac{\partial y_k}{\partial d_k} - w_k\frac{\partial h_k}{\partial d_k}\right) - \sum_{i\in N}(\mu_i^1 - \eta_i^1)\frac{\partial f_i}{\partial d_k}
\end{aligned}$$

Finally, we can derive the derivatives of Lagrange multipliers with time. Using Eqs. (A3), (A4), and (A5), it follows that:

$$\eta_k^1(\iota - \dot{x_k}) = 0 \text{ implies } \dot{\eta_k^1} = \frac{\ddot{x_k}}{\iota - \dot{x_k}}\eta_k^1, \tag{A17}$$

$$\eta_k^2 l_k = 0 \text{ implies } \dot{\eta_k^2} = -\frac{\dot{l_k}}{l_k}\eta_k^2, \text{ and} \tag{A18}$$

$$\eta_k^3(1 - l_k) = 0 \text{ implies } \dot{\eta_k^3} = \frac{\dot{l_k}}{(1-l_k)}\eta_k^3. \tag{A19}$$

A.4 Proof of Proposition 3 and elaboration of Remark 1

Proof of Proposition 3. Let $k \in N$ be a NFP nursing home. Then $k \in N^B$, and $p_k y_k - w_k h_k = 0$. This implies $p_k K^\alpha (1-\theta l_k)^{1-\alpha} - w_k(1-\theta l_k) = 0$. Then, $l_k = \frac{1}{\theta}$ or $l_k = \frac{1}{\theta}\left[1 - \left(\frac{p_k K^\alpha}{w_k}\right)^{\frac{1}{\alpha}}\right]$. For $\theta = 1$, we have $l_k = 1$ or $l_k = 1 - \left(\frac{p_k K^\alpha}{w_k}\right)^{\frac{1}{\alpha}}$. We note that when the capital (K) and the output-price-wage ratio ($\frac{p_k}{w_k}$) are constant over time, the lockdown probability, l_k, is constant over time, and it only depends on the PHSI efficiency θ (given any value of α). When $K < \left(\frac{w_k}{p_k}\right)^{\frac{1}{\alpha}}$, then $1 > \left(\frac{p_k K^\alpha}{w_k}\right)^{\frac{1}{\alpha}}$, and $l_k > 0$. Also, we have $0 \le l_k \le 1$ if and only if $\frac{1-\theta}{K} \le \left(\frac{p_k}{w_k}\right)^{\frac{1}{\alpha}} < \frac{1}{K}$ or $\left(\frac{1-\theta}{K}\right)^{\alpha} \le \frac{p_k}{w_k} < \left(\frac{1}{K}\right)^{\alpha}$. It holds that $\frac{\partial l_k}{\partial \theta} = -\frac{1}{\theta^2} < 0$ or $\frac{\partial l_k}{\partial \theta} = -\frac{1}{\theta^2}\left[1 - \left(\frac{p_k K^\alpha}{w_k}\right)^{\frac{1}{\alpha}}\right] \le 0$.

Further elaborations of Remark 1. Let k be a FP nursing home. Then, $k \in N^A$, and using equation (A14), it holds that:

$$-(1-\alpha)\theta p_k K^{\alpha}(1-\theta l_k(\theta))^{-\alpha} + \theta w_k + \sum_{i\in N}(\mu_i^1 - \eta_i^1)\frac{\partial f_i}{\partial l_k} + \eta_k^2 - \eta_k^3 = 0, \quad \text{(A20)}$$

where,

$$\frac{\partial f_i}{\partial l_k} = -\beta(1-x_i-r_i-d_i)\left[\delta_{ik}\sum_{j\neq i}\mathcal{M}_{ij}(\theta-\theta^2 l_j)x_j + (1-\delta_{ik})(\theta-\theta^2 l_i)\mathcal{M}_{ik}x_k\right].$$

Taking the derivative of Eq. (A20) with respect to θ gives:

$$-(1-\alpha)p_k K^{\alpha}(1-\theta l_k(\theta))^{-\alpha} - \alpha(1-\alpha)\theta p_k K^{\alpha}(l_k+\theta\frac{\partial l_k}{\partial\theta})(1-\theta l_k)^{-\alpha-1} + w_k + \sum_{i\in N}(\frac{\partial\mu_i^1}{\partial\theta} - \frac{\partial\eta_i^1}{\partial\theta})\frac{\partial f_i}{\partial l_k} + \sum_{i\in N}(\mu_i^1-\eta_i^1)\frac{\partial^2 f_i}{\partial\theta\partial l_k} + \frac{\partial\eta_k^2}{\partial\theta} - \frac{\partial\eta_k^3}{\partial\theta} = 0. \quad \text{(A21)}$$

Differentiating $\frac{\partial f_i}{\partial l_k}$ with respect to θ gives:

$$\frac{\partial^2 f_i}{\partial\theta\partial l_k} = \beta\left(\frac{\partial x_i}{\partial\theta} + \frac{\partial r_i}{\partial\theta} + \frac{\partial d_i}{\partial\theta}\right)T_1 - \beta\Big(1-x_i-r_i-d_i\Big)\Big[\delta_{ik}T_2 + (1-\delta_{ik})T_3\Big], \quad \text{(A22)}$$

where,

$$\begin{aligned}
T_1 &= \delta_{ik}\sum_{j\neq i}\mathcal{M}_{ij}(\theta-\theta^2 l_j)x_j + (1-\delta_{ik})(\theta-\theta^2 l_i)\mathcal{M}_{ik}x_k \\
T_2 &= \sum_{j\neq i}\mathcal{M}_{ij}\left[\left(1-2\theta l_j-\theta^2\frac{\partial l_j}{\partial\theta}\right)x_j + (\theta-\theta^2 l_j)\frac{\partial x_j}{\partial\theta}\right] \\
T_3 &= \mathcal{M}_{ik}\left[\left(1-2\theta l_i-\theta^2\frac{\partial l_i}{\partial\theta}\right)x_k + (\theta-\theta^2 l_i)\frac{\partial x_k}{\partial\theta}\right]
\end{aligned}$$

Substituting Eq. (A22) into Eq. (A21), we obtain an implicit equation including the derivative of the lockdown probability l_k with θ, $\frac{\partial l_k}{\partial\theta}$, and other derivatives of lockdown probability l_j with θ, $\frac{\partial l_j}{\partial\theta}$, for $j \neq k$. It follows that for all $k \in N^A$, we can not conclude whether $\frac{\partial l_k}{\partial\theta}$ is positive, negative, or null. In fact, if we assume

$$\frac{\partial\mu_i^1}{\partial\theta} = \frac{\partial\eta_i^1}{\partial\theta} = \frac{\partial^2 f_i}{\partial\theta\partial l_k} = \frac{\partial\eta_k^2}{\partial\theta} = \frac{\partial\eta_k^3}{\partial\theta} = 0 \text{ for all } \forall i \in N \text{ and } k \in N^A,$$

then Eq. (A21) becomes:

$$-(1-\alpha)p_k K^{\alpha}(1-\theta l_k(\theta))^{-\alpha} - \alpha(1-\alpha)\theta p_k K^{\alpha}(l_k+\theta\frac{\partial l_k}{\partial\theta})(1-\theta l_k)^{-\alpha-1} + w_k = 0.$$

Then, we can express the derivative of lockdown with PHSI efficiency level θ as

$$\frac{\partial l_k}{\partial\theta} = \frac{w_k - (1-\alpha)p_k K^{\alpha}(1-\theta l_k)^{-\alpha-1}(1-\theta l_k(1-\alpha))}{\alpha\theta^2(1-\alpha)p_k K^{\alpha}(1-\theta l_k)^{-\alpha-1}}. \quad \text{(A23)}$$

Since $(1-\alpha)p_k K^{\alpha}(1-\theta l_k)^{-\alpha-1}(1-\theta l_k(1-\alpha)) \geq 0$, then from Eq. (A23), it is direct that the sign of $\frac{\partial l_k}{\partial\theta}$ can be either positive or negative depending on whether the wage w_k is greater or less than $(1-\alpha)p_k K^{\alpha}(1-\theta l_k)^{-\alpha-1}(1-\theta l_k(1-\alpha))$.

Appendix B Additional tables

Table B1: Calibrated and estimated parameters sources and descriptions at U.S. state level

Parameters or Variables	Value	Definitions and Sources	Utilization
Epidemiological			
β	$\frac{R_0}{18}$	The COVID-19 reproduction numbers R_0 estimated during April to July 2020, from Statista	Calibration
γ	(1-death/case)/18	case and death per 1000 in nursing homes in each U.S. state as of Sep. 2020 from Statista	Calibration
κ	(death/case)/18	case and death per 1000 for in nursing homes in each U.S. state as of Sep. 2020 Statista	Calibration
Raw data Death Count	COVID-19 death	CMS data May 31 to August 16, 2020	Calibration
$\mathcal{M}$	Network of nursing homes	Protect Nursing Home Project	Calibration and Estimations
Economic			
For profit Indicator	Dummy variable indicating a nursing home's ownership (FP or NFP)	Replication data from Chen et al. (2021)	Calibration
Capital	Number of beds in the nursing home	Replication data from Chen et al. (2021)	Calibration
Price	Average hourly cost of a Private Room	Senior Living Project	Calibration
Wage	Average hourly wage by U.S. state	Bureau of Labor Statistics	Calibration
α	Cobb-Douglass production function	Replication data from Chen et al. (2021) and authors' estimations for each U.S state	Calibration
Regressions Tables	Variables	Replication data from Chen et al. (2021) and authors' calculations	Estimations

Table B2: Effects of PHSI efficiency and other OxCGRT indexes on COVID-19 deaths in U.S. nursing homes

	(1)	(2)	(3)	(4)	(5)	(6)
θ	-12.12***	-12.46***	-12.65***	-12.74***	-11.91***	-12.87***
	(-6.64)	(-7.12)	(-7.20)	(-7.21)	(-6.57)	(-7.25)
Eig_Cent	2.428***	2.271***	2.402***	2.257***	2.441***	2.319***
	(3.88)	(3.66)	(3.87)	(3.65)	(3.93)	(3.74)
County_ses	0.00641***	0.00611***	0.00532***	0.00577***	0.00523***	0.00535***
	(5.72)	(5.47)	(4.98)	(5.24)	(4.91)	(5.00)
Workplaces	0.0660	0.101**	0.123***	0.123***	0.0972**	0.137***
	(1.43)	(2.30)	(2.67)	(2.65)	(1.97)	(2.84)
D_Profit	-0.425***	-0.542***	-0.400**	-0.543***	-0.348**	-0.473***
	(-2.65)	(-3.34)	(-2.53)	(-3.37)	(-2.18)	(-2.91)
$\theta\times$ Workplaces	-0.455***	-0.461***	-0.472***	-0.470***	-0.448***	-0.477***
	(-6.81)	(-7.20)	(-7.30)	(-7.28)	(-6.74)	(-7.33)
$\theta\times$ D_Profit	1.287***	1.481***	1.291***	1.498***	1.193***	1.406***
	(4.19)	(4.78)	(4.36)	(4.87)	(3.92)	(4.57)
$\theta\times$ Eig_Cent	2.528**	2.878**	2.602**	2.915**	2.528**	2.783**
	(2.09)	(2.38)	(2.18)	(2.42)	(2.12)	(2.33)
$\theta\times$ County_ses	-0.00185***	-0.00135***	-0.00196***	-0.00136***	-0.00211***	-0.00166***
	(-4.09)	(-2.87)	(-4.38)	(-2.96)	(-4.65)	(-3.49)
Overall Rating	-0.191***	-0.188***	-0.185***	-0.185***	-0.186***	-0.184***
	(-4.39)	(-4.31)	(-4.23)	(-4.25)	(-4.26)	(-4.20)
Governor Approval	0.0657***	0.0556***	0.0733***	0.0574***	0.0769***	0.0663***
	(9.38)	(7.64)	(10.38)	(7.99)	(11.04)	(9.41)
Stringency Index	0.00992				-0.0216**	
	(0.96)				(-2.43)	
Containment Health Index		0.0563***				0.0290**
		(3.91)				(2.22)
Economic Support Index			0.0268***		0.0308***	0.0221***
			(4.39)		(5.08)	(3.72)
Government Response Index				0.0647***		
				(4.34)		
Constant	-0.800	-2.054*	-0.917	-2.122**	-0.761	-1.571
	(-0.74)	(-1.96)	(-0.85)	(-2.04)	(-0.70)	(-1.46)
Observations	11406	11406	11406	11406	11406	11406
R^2	0.096	0.098	0.098	0.098	0.099	0.099

Notes: Data are from the CMS as of May 31, 2020, Chen et al. (2021), Hale et al. (2021), Google's Community Mobility Reports (CMR, 2020), and authors' estimations. The dependent variable is the number of COVID-19 deaths among residents in a nursing home. t statistics in parentheses. $^{*}p < 0.1$, $^{**}p < 0.05$, $^{***}p < 0.01$.

References

Akhtar-Danesh, N., Baumann, A., Crea-Arsenio, M., Antonipillai, V. (2022). Covid-19 excess mortality among long-term care residents in Ontario, Canada. *Plos One*, *17*(1), e0262807.

Assob-Nguedia, J.-C., Dongo, D., Nguimkeu, P.E. (2020). Early dynamics of transmission and projections of COVID-19 in some west african countries. *Infectious Disease Modelling*, *5*, 839–847.

Bach-Mortensen, A.M., Verboom, B., Movsisyan, A., Degli Esposti, M. (2021). A systematic review of the associations between care home ownership and covid-19 outbreaks, infections and mortality. *Nature Aging*, *1*(10), 948–961.

Ballester, C., Calvó-Armengol, A., Zenou, Y. (2006). Who's who in networks. wanted: The key player. *Econometrica*, *74*(5), 1403–1417.

Banerjee, A., Chandrasekhar, A.G., Duflo, E., Jackson, M.O. (2013). The diffusion of microfinance. *Science*, *341*(6144).

Bartscher, A.K., Seitz, S., Siegloch, S., Slotwinski, M., Wehrhöfer, N. (2021). Social capital and the spread of Covid-19: Insights from European countries. *Journal of Health Economics*, *80*, 102531.

Battiston, P., & Stanca, L. (2015). Boundedly rational opinion dynamics in social networks: Does indegree matter? *Journal of Economic Behavior & Organization*, *119*, 400–421.

Baumeister, C., Leiva-León, D., Sims, E. (2024). Tracking weekly state-level economic conditions. *Review of Economics and Statistics*, 1–22.

Bosi, S., Camacho, C., Desmarchelier, D. (2021). Optimal lockdown in altruistic economies. *Journal of Mathematical Economics*, *93*, 102488.

Boucekkine, R., Carvajal, A., Chakraborty, S., Goenka, A. (2021). The economics of epidemics and contagious diseases: An introduction. *Journal of Mathematical Economics*, *93*, 102498.

Buechel, B., Hellmann, T., Klößner, S. (2015). Opinion dynamics and wisdom under conformity. *Journal of Economic Dynamics and Control*, *52*, 240–257.

Bui, D.P. (2020). Association between cms quality ratings and covid-19 outbreaks in nursing homes—west virginia, march 17–june 11, 2020. *MMWR. Morbidity and mortality weekly report*, *69*.

Callaway, B., & Li, T. (2023). Evaluating policies early in a pandemic: Bounding policy effects with nonrandomly missing data. *Review of Economics and Statistics*, 1–45.

Caulkins, J.P., Grass, D., Feichtinger, G., Hartl, R.F., Kort, P.M., Prskawetz, A., ... Wrzaczek, S. (2021). The optimal lockdown intensity for COVID-19. *Journal of Mathematical Economics*, *93*, 102489.

Chen, M.K., Chevalier, J.A., Long, E.F. (2021). Nursing home staff networks and COVID-19. *Proceedings of the National Academy of Sciences*, *118*(1).

Cheng, C., Messerschmidt, L., Bravo, I., Waldbauer, M., Bhavikatti, R., Schenk, C., ... Barceló, J. (2024). Harmonizing government responses to the COVID-19 pandemic. *Scientific Data*, *11*(1), 204.

CMR (2020). *Google community mobility reports.* Retrieved from https://www.google.com/covid19/mobility/ (Accessed: 2023-04-17)

Conlen, M., Ivory, D., Yourish, K., Lai, R., Hassan, A., Calderone, J. (2021). *Nearly one-third of U.S. coronavirus deaths are linked to nursing homes.* (Accessed at https://www.nytimes.com/interactive/2020/us/coronavirus-nursing-homes.html)

Cronin, C.J., & Evans, W.N. (2021). Total shutdowns, targeted restrictions, or individual responsibility: How to promote social distancing in the COVID-19 era? *Journal of Health Economics*, *79*, 102497.

Cronin, C.J., & Evans, W.N. (2022). Nursing home quality, COVID-19 deaths, and excess mortality. *Journal of Health Economics*, *82*, 102592.

Debnam Guzman, J., Mabeu, M.C., Pongou, R. (2022). Identity during a crisis: COVID-19 and ethnic divisions in the United States. *AEA Papers and Proceedings*, *112*, 319-–324.

Di Porto, E., Naticchioni, P., Scrutinio, V. (2022). Lockdown, essential sectors, and Covid-19: Lessons from Italy. *Journal of Health Economics*, *81*, 102572.

Dykgraaf, S.H., Matenge, S., Desborough, J., Sturgiss, E., Dut, G., Roberts, L., ... Kidd, M. (2021). Protecting nursing homes and long-term care facilities from covid-19: a rapid review of international evidence. *Journal of the American Medical Directors Association*, *22*(10), 1969–1988.

Eichenbaum, M.S., Rebelo, S., Trabandt, M. (2022). Epidemics in the New Keynesian model. *Journal of Economic Dynamics and Control*, 104334.

Federico, S., & Ferrari, G. (2021). Taming the spread of an epidemic by lockdown policies. *Journal of Mathematical Economics*, *93*, 102453.

Fernández-Villaverde, J., & Jones, C.I. (2022). Estimating and simulating a SIRD model of COVID-19 for many countries, states, and cities. *Journal of Economic Dynamics and Control*, 104318.

Forneron, J.-J., & Ng, S. (2018). The ABC of simulation estimation with auxiliary statistics. *Journal of Econometrics*, *205*(1), 112–139.

Fuxian, L., Liu, Q., Pei, M., Qian, N., Wei, S.-J., Zhang Huyue, A. (2022). The Zero-COVID revolution? *Project Syndicate*. Retrieved from https://www.project-syndicate.org/onpoint/the-zero-covid-revolution (Accessed: 2023-01-18)

Galeotti, A., Golub, B., Goyal, S. (2020). Targeting interventions in networks. *Econometrica*, *88*(6), 2445–2471.

Gebhard, C., Regitz-Zagrosek, V., Neuhauser, H.K., Morgan, R., Klein, S.L. (2020). Impact of sex and gender on covid-19 outcomes in europe. *Biology*

of sex differences, *11*, 1–13.

Gertler, P.J., & Waldman, D.M. (1992). Quality-adjusted cost functions and policy evaluation in the nursing home industry. *Journal of Political Economy*, *100*(6), 1232–1256.

Giri, S., Chenn, L.M., Romero-Ortuno, R. (2021). Nursing homes during the COVID-19 pandemic: a scoping review of challenges and responses. *European Geriatric Medicine*, *12*(6), 1127–1136.

Gollier, C. (2020). Cost–benefit analysis of age-specific deconfinement strategies. *Journal of Public Economic Theory*, *22*(6), 1746–1771.

Gorges, R.J., & Konetzka, R.T. (2020). Staffing levels and covid-19 cases and outbreaks in us nursing homes. *Journal of the American Geriatrics Society*, *68*(11), 2462–2466.

Gupta, A., Howell, S.T., Yannelis, C., Gupta, A. (2021). *Does private equity investment in healthcare benefit patients? evidence from nursing homes* (Tech. Rep.). National Bureau of Economic Research.

Gutierrez, E., & Rubli, A. (2021). Shocks to hospital occupancy and mortality: Evidence from the 2009 h1n1 pandemic. *Management Science*, *67*(9), 5943–5952.

Hale, T., Angrist, N., Goldszmidt, R., Kira, B., Petherick, A., Phillips, T., ... Tatlow, H. (2021). A global panel database of pandemic policies (Oxford COVID-19 Government Response Tracker). *Nature Human Behaviour*, *5*(4), 529–538.

Harrington, C., Ross, L., Chapman, S., Halifax, E., Spurlock, B., Bakerjian, D. (2020). Nurse staffing and coronavirus infections in california nursing homes. *Policy, Politics, & Nursing Practice*, *21*(3), 174–186.

Herz, H., Kistler, D., Zehnder, C., Zihlmann, C. (2024). Hindsight bias and trust in government. *Review of Economics and Statistics*, 1–30.

Ioannidis, J.P., Axfors, C., Contopoulos-Ioannidis, D.G. (2021). Second versus first wave of COVID-19 deaths: shifts in age distribution and in nursing home fatalities. *Environmental Research*, *195*, 110856.

Li, Y., Cen, X., Cai, X., Temkin-Greener, H. (2020). Racial and ethnic disparities in covid-19 infections and deaths across us nursing homes. *Journal of the American Geriatrics Society*, *68*(11), 2454–2461.

Lloyd, A.L., Valeika, S., Cintrón-Arias, A. (2006). Infection dynamics on small-world networks. *Contemporary Mathematics*, *410*, 209–234.

Londoño-Vélez, J., & Querubin, P. (2022). The impact of emergency cash assistance in a pandemic: Experimental evidence from colombia. *Review of Economics and Statistics*, *104*(1), 157–165.

Makris, M. (2021). Covid and social distancing with a heterogenous population. *Economic Theory*, 1–50.

Marquez-Padilla, F., & Saavedra, B. (2022). The unintended effects of the COVID-19 pandemic and stay-at-home orders on abortions. *Journal of Population Economics*, *35*(1), 269–305.

Nganmeni, Z., Pongou, R., Tchantcho, B., Tondji, J.-B. (2022). Vaccine and inclusion. *Journal of Public Economic Theory*, *Forthcoming*.

Nguimkeu, P., & Tadadjeu, S. (2021). Why is the number of COVID-19 cases lower than expected in Sub-Saharan Africa? a cross-sectional analysis of the role of demographic and geographic factors. *World Development*, *138*, 105251.

O'Neill, C., Harrington, C., Kitchener, M., Saliba, D. (2003). Quality of care in nursing homes: An analysis of relationships among profit, quality, and ownership. *Medical care*, 1318–1330.

Palomino, J.C., Rodríguez, J.G., Sebastian, R. (2020). Wage inequality and poverty effects of lockdown and social distancing in europe. *European Economic Review*, *129*, 103564.

Pastor-Satorras, R., Castellano, C., Van Mieghem, P., Vespignani, A. (2015). Epidemic processes in complex networks. *Reviews of Modern Physics*, *87*(3), 925.

Pestieau, P., & Ponthiere, G. (2022). Optimal lockdown and social welfare. *Journal of Population Economics*, *35*, 241–268.

Pindyck, R.S. (2020). *Covid-19 and the welfare effects of reducing contagion* (Tech. Rep.). National Bureau of Economic Research.

Pongou, R., & Serrano, R. (2013). Fidelity networks and long-run trends in HIV/AIDS gender gaps. *American Economic Review*, *103*(3), 298–302.

Pongou, R., Tchuente, G., Tondji, J.-B. (2022). Laissez-faire, social networks, and race in a pandemic. *AEA Papers and Proceedings*, *112*, 325—329.

Pongou, R., Tchuente, G., Tondji, J.-B. (2023). Optimal Interventions in Networks during a Pandemic. *Journal of Population Economics*, *36*(2), 847–883.

Pongou, R., & Tondji, J.-B. (2018). Valuing inputs under supply uncertainty: The bayesian Shapley value. *Games and Economic Behavior*, *108*, 206–224.

Spector, W.D., Selden, T.M., Cohen, J.W. (1998). The impact of ownership type on nursing home outcomes. *Health Economics*, *7*(7), 639–653.

Young, H.P. (2009). Innovation diffusion in heterogeneous populations: Contagion, social influence, and social learning. *American Economic Review*, *99*(5), 1899–1924.

Young, H.P. (2011). The dynamics of social innovation. *Proceedings of the National Academy of Sciences*, *108*(Supplement 4), 21285–21291.

Zhao, N., Yao, S., Thomadsen, R., Wang, C.B. (2024). The impact of government interventions on covid-19 spread and consumer spending. *Management Science*, *70*(5), 3302–3318.